

We are committed to providing [accessible customer service](#).

If you need accessible formats or communications supports, please [contact us](#).

Nous tenons à améliorer [l'accessibilité des services à la clientèle](#).

Si vous avez besoin de formats accessibles ou d'aide à la communication, veuillez [nous contacter](#).

CRITICAL RESOURCES LTD
MAVIS LAKE PROJECT
LITHO-STRUCTURAL INTERPRETATION OF AIRBORNE
GEOPHYSICAL DATA
Conducted By:



SOUTHERN GEOSCIENCE
CONSULTANTS

APRIL, 2022

SGC4007

Report Edited By:
Troy Gallik P. Geo
Exploration Manager of:



November 23 2022

Client: Critical Resources Ltd.	Project(s): Mavis Lake
Report Number: SGC4007	Date: 29 th April 2022
Compiled By: Pavel Jurza, Principal Geophysicist, pavel.jurza@sgc.com.au	
Author(s): Pavel Jurza	
Peer Reviewed By: Bill Peters, Senior Consulting Geophysicist, bill.peters@sgc.com.au	
Assessment Report Edited and Submitted By: Troy Gallik P.Geo of Critical Resources Limited	
Key words: Canada, Ontario, lithium deposits, pegmatite, interpretation, airborne magnetics	
Commodity: Lithium	
Province / State, Country: Superior Province, Ontario, Canada	
1:100,000 map sheet(s):	
1:250,000 map sheet(s):	

CONTENTS

CONTENTS	ii
LIST OF FIGURES.....	iii
LIST OF TABLES.....	iii
LIST OF PLANS.....	iii
ABBREVIATIONS.....	iv
SUMMARY	v
1 INTRODUCTION.....	1
1.1 Previous Work.....	1
2 GEOLOGICAL SETTING.....	2
3 SURVEY DETAILS.....	3
3.1 Magnetic data	3
3.2 Radiometric data.....	3
3.3 VLF data.....	4
4 INTERPRETATION	5
4.1 Method.....	5
4.2 Litho-structural interpretation.....	6
4.3 Targeting	7
5 CONCLUSIONS AND RECOMMENDATIONS	10
6 REFERENCES.....	12
PLANS AND APPENDIX.....	13

LIST OF FIGURES

Figure 1: Location map showing Mavis Lake project. Critical tenements shown in magenta, airborne survey outline shown in yellow. Sentinel-2 RGB natural image (2021) shown in the background.	1
Figure 2: Project geology (after Berdusco, 2000). Tenements are shown as red and ground magnetics survey outline as green polygons. Legend: undifferentiated granite/ gneiss (6a, 6b) is pink, mafic metavolcanics (1a) are green and metasediments (3) are grey.	2
Figure 3: Magnetic RTP-2VD image (LEFT) and radiometric K-Th-U RGB ternary image (RIGHT).....	3
Figure 4: DEM image (LEFT) and high-resolution RGB natural colour satellite imagery (RIGHT).....	4
Figure 5: VLF – Total Field-LINE component (LEFT) and VLF-Total Field-ORTHO component (RIGHT) images. Note that LINE and ORTHO signals are linked to transmitters at different directions from the AOI highlighting structures with different strikes.	4
Figure 6: Litho-structural interpretation of Mavis Lake project area.....	7
Figure 7: Radiometric potassium concentration image (LEFT) and potassium/thorium ratio image (RIGHT) with basic lithological boundaries (black polygons) and known pegmatite occurrences (magenta symbols) in the overlay. There is no significant correlation between pegmatite occurrences and radiometric anomalies or lithological blocks (except maybe for granites).....	8

LIST OF TABLES

Table 1: Summary of the airborne survey.	3
Table 2: List of target areas	9

LIST OF PLANS

- Plan 1: Litho-structural interpretation
- Plan 2: Litho-structural interpretation with targets
- Plan 3: Structural interpretation over magnetic image
- Plan 4: VLF Conductive Axes over VLF Total Field-derivative image
- Plan 5: Targets and radiometric anomalies over Potassium image

ABBREVIATIONS

SGC	Southern Geoscience Consultants
Critical	Critical Resources Limited (Company)
Li	Lithium
Ta	Tantalum
Be	Beryllium
Cs	Caesium
DEM	digital elevation model
GIS	Geographic Information System
1VD	First vertical derivative
2VD	Second vertical derivative
RTP	reduced-to-pole
TMI	Total Magnetic Intensity
UTM	Universal Transverse Mercator
SGC	Southern Geoscience Consultants

SUMMARY

Geophysical, geological, and other supportive information over the Mavis Lake Project have been processed and analysed by Southern Geoscience Consultants (SGC) on behalf of Critical Resources Limited (Critical) to identify lithium bearing pegmatite targets. A total of \$143004 worth of expenses were accumulated from the survey and the data interpretation.

The Project has excellent road accessibility that is approximately 19 km northeast by road from the city of Dryden and can be reached from the city by driving east on Trans-Canada Highway 17 for approximately 8km to its junction with the Thunder Lake Road. On Thunder Lake Road travel is roughly 3km to the intersection of Thunder Lake Road and Ghost Lake South Road. From this point, driving north on the Ghost Lake South Road for about 1km and thence turn east along an old logging road, a major gravel road, for approximately 1km brings one to an intersection to the main access road to the Fairservice Mining Leases. Continuing along the Fairservice access road for an additional 3km brings the driver to a subsidiary gravel north to the eastern claims of the Mavis Lake property. Central location of the property is 524650E 5517917N WGS 1984 UTM Zone 15N.

At Mavis Lake, the litho-structural, 1:10,000 scale interpretation was based on processing and analysis of recent airborne geophysical survey data conducted by MPX Geophysics Ltd from November 1st to November 10th, 2021. Survey data included magnetic, radiometric, VLF and DEM data. The interpretation was based, however, mostly on magnetic data which contains useful information regarding the underlying geology and structure of the project area, revealing complex basement geology consisting of metasediments and deformed volcanic belts including ultramafic, mafic and felsic lithologies. Granitoid bodies believed to be important in the pegmatite formation process were outlined. Prominent regional trends as well as structures were interpreted using magnetic and VLF data.

The targeting process was based on structural and lithological information provided by interpretation. Although, geophysical data alone does not support direct targeting of pegmatites, a strategy based on lithological associations, structural context/complexity, reduction of the search area and knowledge of pegmatite occurrences has been used. Based on the data interpretation and information available to SGC, 28 target areas for lithium pegmatites have been selected for follow up.

For initial follow up of the targets, reconnaissance drilling, geochemical sampling and geological mapping has been recommended.

At the detailed scale, the cost of geophysics must be balanced against the cost of simple exploratory shallow drilling. Geophysical methods that may work are magnetics, radiometrics, gravity, galvanic resistivity, induced polarisation, ground probing radar, shallow seismics, and sub-audio magnetotellurics (SAM). If any of these are proven, they could be used to trace known pegmatites under cover and to locate additional pegmatites. Physical property testing of core samples has been strongly recommended prior to further ground surveys to establish the best geophysical approaches.

1 INTRODUCTION

Critical Resources (Critical) has asked Southern Geoscience Consultants (SGC) to compile, process and interpret magnetic, radiometric and DEM data acquired over their Mavis Lake lithium project, based in the Superior Province of Ontario, Canada. The main objective of the interpretation work was to assist with targeting for lithium-bearing pegmatites. A larger plan map and claims list are located in Appendix B and C.

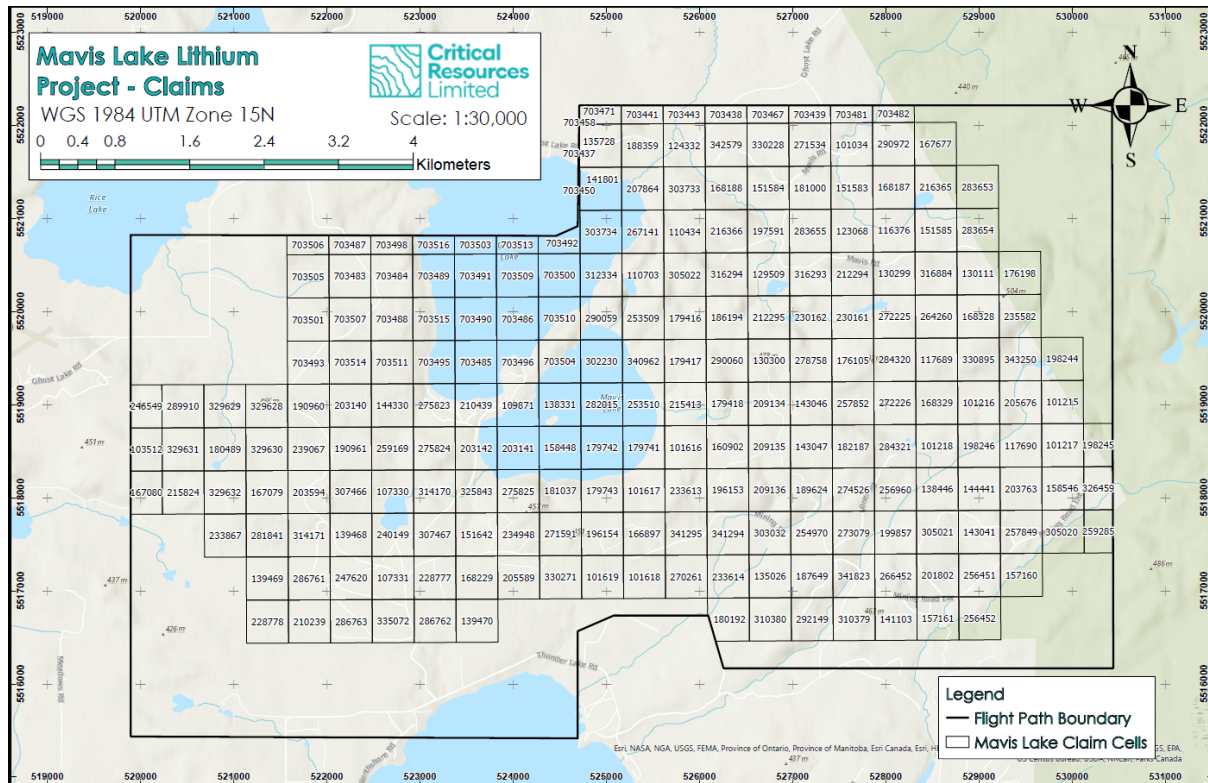


Figure 1: Location map showing Mavis Lake project. Critical tenements shown as black squares with claim ID labeled, airborne survey boundary shown in bold black.

The interpretation primarily utilised a 2021 magnetic/radiometric survey dataset flown at 75m line spacing and 70m ground clearance (which is higher than today’s usual ground clearance 35-50m) that covers the whole project area, along with all relevant and available auxiliary information. This airborne dataset was previously processed by SGC to produce a full set of images and vectors. Flight path is located in Plans section.

1.1 Previous Work

Current work based on airborne geophysical data was preceded by interpretation of ground magnetics data completed by SGC in 2018 (Wallace 2018) for Pioneer Resources, which also included comprehensive assessment of drilling and geochemistry data. Geophysical, drilling and geochemistry information gathered within the scope of 2018 interpretation work was utilized for the benefit of the current airborne data interpretation.

It should be noted that ground and airborne data (flown over Mavis Lake project at 70m) differ. As a trade-off, the ground data can have higher resolution, however, they are more susceptible to surface and instrument related magnetic noise and tend to highlight shallower magnetic sources. Airborne data, on the other hand, are better at natural filtering of the surface noise and therefore are better in capturing continuity of magnetic units. With increased clearance, however, more natural data smoothing/averaging is present in

the airborne data. For these reasons, interpretations of ground and airborne data may not be exactly the same in the detail. As the current interpretation work was based on airborne data, the airborne data interpretation was given higher priority over older ground data interpretation in cases of disagreement.

2 GEOLOGICAL SETTING

The following information was taken from Wallace 2018.

The geology of the Mavis Lake property, located in the collisional Sioux Lookout Domain of the western Wabigoon sub-province, is included in a report by Clark *et. al.* (2009) and Map 2115 (Kenora-Fort Frances Sheet) from a geological compilation by Berdusco (2000). The project is located approximately 4km north of the major Wabigoon Fault Zone, trending east-west in this area, on the north limb of a westerly plunging syncline, adjacent to the Thunder Lake Anticline. The tenement comprises multiply folded metasediments and mafic metavolcanics, a granite batholith body in the northwest (Ghost Lake/ Mavis Lake), and intrusions of ultramafic dikes, gabbro sills and stocks and numerous granite pegmatite dikes

Granitic pegmatites and associated metasomatic zones of the Mavis Lake pegmatite group (MPG) are likely genetically related to the Ghost Lake Batholith (GLB) and extend approximately 2 × 8 kilometres in dimension (Clark *et. al.* 2009). The Li-Cs-Ta mineralised dykes are between 11 and 250 metres in length and up to several metres in width. The majority of the pegmatites strike parallel to the host rock foliation and show localised effects of late tectonic deformation. Those in the outer zones, however, post-date the tectonic deformation and show discordant emplacement, and lack of ductile deformation features.

Figure 2 shows the Mavis Lake local geology.

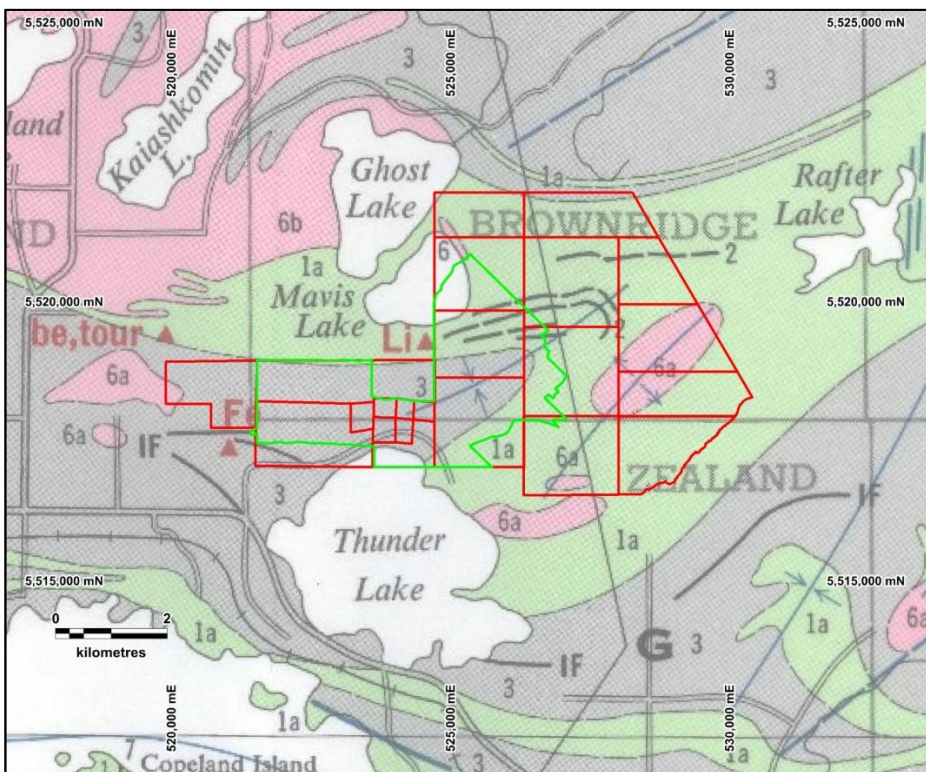


Figure 2: Project geology (after Berdusco, 2000). Legacy tenements are shown as red and ground magnetic survey outline as green polygons. Legend: undifferentiated granite/ gneiss (6a, 6b) is pink, mafic metavolcanics (1a) are green and metasediments (3) are grey.

3 SURVEY DETAILS

Data processing of the 2021 Mavis Lake/Dryden Block survey was completed by SGC in January 2022. Final products were delivered in a MapInfo-compatible format using the WGS84 datum and NUTM Zone 15 projection. Survey details are presented in Appendix A.

Table 1: Summary of the airborne survey.

SURVEY NAME	METHODS	JOB #	CONTRACTOR	SURVEY YEAR	FLIGHT LINE SPACING (metres)	MEAN TERRAIN CLEARANCE (metres)	FLIGHT LINE DIRECTION (degrees)	DATA STATUS
Mavis Lake / Dryden Block	MAG RAD VLF DEM	P21084	MPX Geophysics Ltd	2021	75	70	000 - 180	Confidential

3.1 Magnetic data

The magnetic data are of average quality, not top quality as would be in the case of a detailed survey at 50m line spacing and flown with 35-50m ground clearance. The magnetic data were primary source of interpretation.

3.2 Radiometric data

Radiometric data were acquired, however having insufficient correlation with the expected bedrock geology or known pegmatite occurrences were not much used in the interpretation. The high correlation between Potassium, Uranium and Thorium concentrations (as demonstrated by the ternary image in Figure 3 - right) significantly reduces the usefulness of radiometric ratios or ternary images and is a sign that the radiometric data is influenced more by forest soils, vegetation and environmental factors rather than by variations in bedrock geology. In line with those observations, the possible correlation of radiometric data with recent forest clearings was assessed with the help of recent (2021) Sentinel-2 imagery. However, local increases in radiometric concentrations correlate with places of forest clearings only weakly.

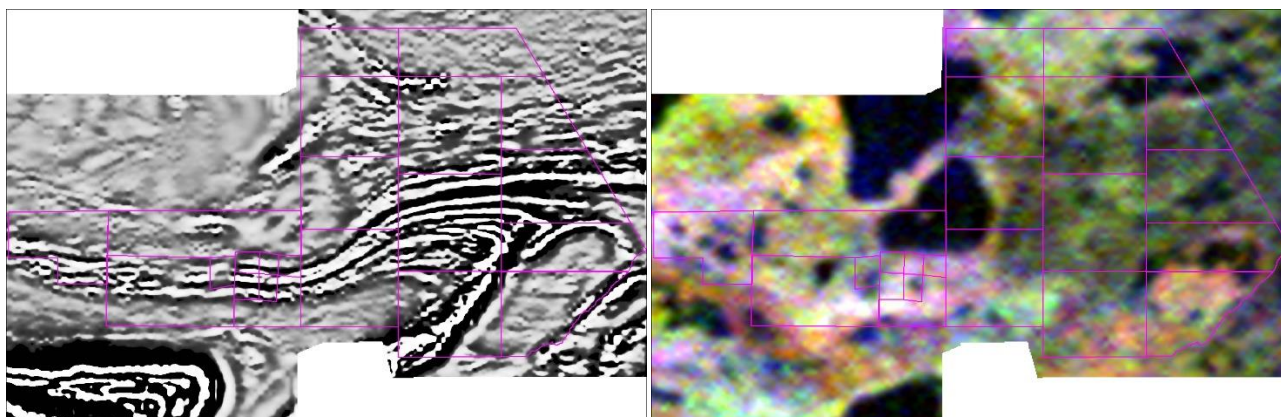


Figure 3: Magnetic RTP-2VD image (LEFT) and radiometric K-Th-U RGB ternary image (RIGHT).

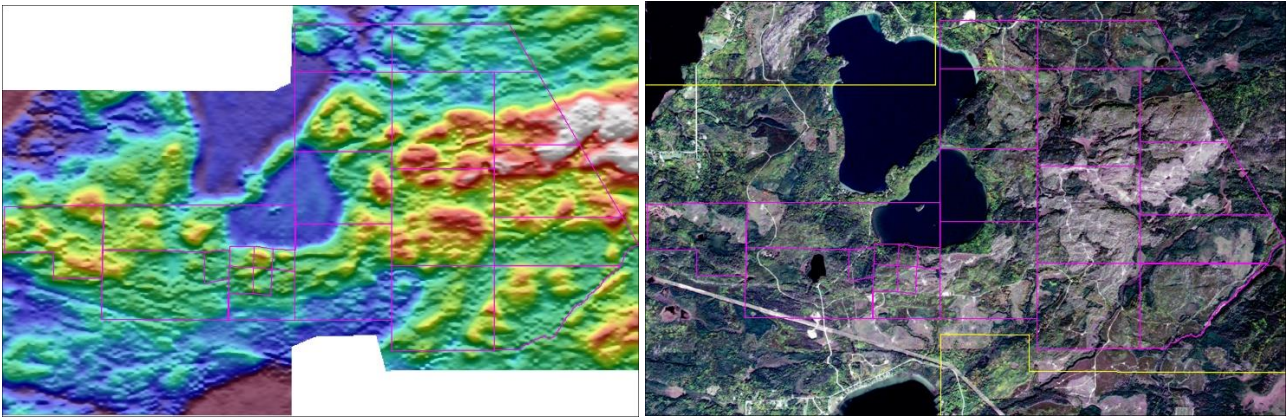


Figure 4: DEM image (LEFT) and high-resolution RGB natural colour satellite imagery (RIGHT)

3.3 VLF data

Also collected were VLF data using a TOTEM VLF instrument. The Totem 2 VLF-EM system uses three orthogonal receiver coils (LINE, ORTHO, ERECT) to derive the total field and vertical quadrature component of the signal from two VLF transmitters. These transmitters should be in different directions from the surveyed area in order to provide optimum coupling to conductors with different strike directions.

The principal antenna for **LINE** is aligned with the flight direction, **ORTHO** is transverse to the flight line direction and **ERECT** is in vertical direction. The Totem system designates the measured signals as **LINE** and **ORTHO**, each with a *total field* and *vertical quadrature component*.

Total Field: The signal in the principal antenna (LINE or ORTHO) is used to define in-phase components. The vector sum of the in-phase components from the three orthogonal coils is calculated and scaled with respect to a user established background signal level to provide "total field" as percent variation.

Quadrature: The signal in the vertical antenna, in quadrature with the phase established by the principal antenna (LINE or ORTHO) is the scaled to provide "vertical quadrature", as percent variation.

Images of two Total Field components are shown in Figure 5.

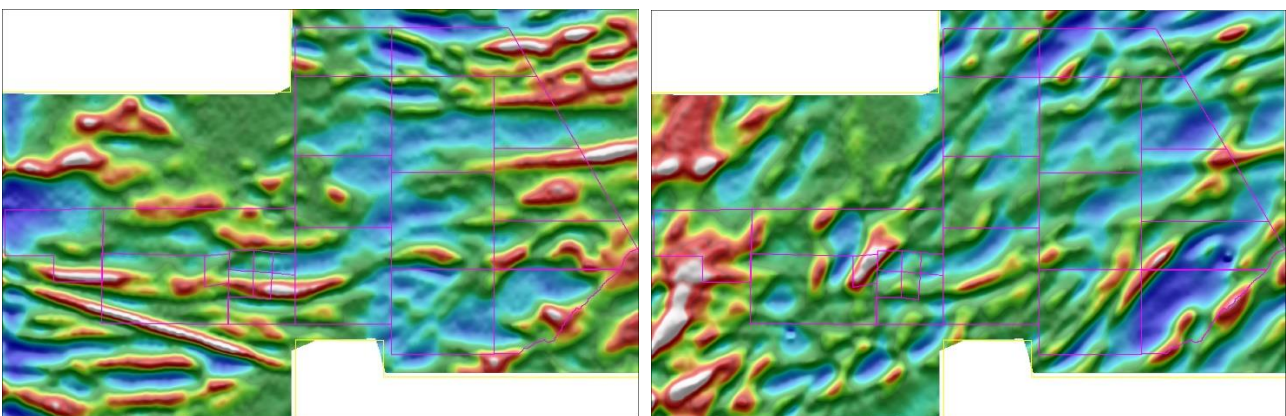


Figure 5: VLF – Total Field-LINE component (LEFT) and VLF-Total Field-ORTHO component (RIGHT) images. Note that LINE and ORTHO signals are linked to transmitters at different directions from the AOI highlighting structures with different strikes.

VLF data have been interpreted and VLF-based conductive axes were delineated for individual VLF products (Total Field-LINE, Total Field-ORTHO, Quadrature-LINE and Quadrature-ORTHO). Fraser filtering was applied to quadrature data prior interpretation.

Apart from obvious cultural sources, it is likely that many of the VLF conductor axes may be related to conductive overburden and are not reflective of the underlying geology or structure of interest. Axes that are reflected in both the magnetic and VLF data are most likely of structural/bedrock origin. Over the Mavis Lake project area, the VLF conductive axes agree very well with both principal geological trends (in E-W and SW-NE direction) as discussed in chapter 4.2 and have been utilized within the complex of other methods (mainly magnetics) in litho-structural interpretation of the area.

4 INTERPRETATION

Interpretation work has been based primarily on the interrogation of the **magnetic data**, with assistance from the **VLF data** (the contribution discussed above in chapter 3.3), as well as from available drill hole and geochemistry data supplied by Critical or taken from Wallace 2018. Interpretation of VLF data is provided in a separate GIS layer (VLF_conductive axes).

Radiometric data were not utilized much for reasons discussed in the chapters 3.2 and 4.3. As a possibly useful product in future investigations, *Potassium concentration* and *Potassium/Thorium ratio* anomalies were outlined and provided as individual GIS layers.

Information about **solid geology** was taken from various sources (such as Berdusco 2000, Clark 2009) or from available drill information. Satellite data have been used to cross check for suspected cultural origins of some of the magnetic anomalies and for an assessment of vegetation cover. **DEM data** were also analysed; however, they did not seem to produce any important leads for interpretation or targeting.

All work was done in the North UTM Zone 15/WGS84 projection at an output scale of 1:10 000, however the primary structure and unit delineation was carried out at about 1:6 000 scale before conversion to the final GIS product. MapInfo and ArcGIS vector layers and scaled PDF plans were produced.

4.1 Method

Derivatives of reduced-to-pole (RTP) magnetic data (half, first and second vertical derivative or analytical signal and tilt angle) have been used to interpret structural features. These derivatives show more detail than the TMI and RTP TMI images.

Fractures, minor faults and secondary faults are not usually directly visible in the magnetic data (especially over sedimentary complexes) however they are inferred from the greater structural context, as they displace or break the magnetic response of geological units or lithological contacts. This is very much the case over areas covered by weakly magnetic (meta) sedimentary, volcanic complexes or non-magnetic intrusions. However, faults and fractures have been inferred with reasonable confidence within strongly magnetic domains, such as mafic volcanic sequences and complexes.

4.2 Litho-structural interpretation

The Mavis Lake interpretation is shown in Figure 6. The central part (as well as both SW and SE corners) of the interpretation area (AOI) comprises a heavily deformed belt containing layered felsic and mafic volcanics with strongly magnetic ultramafic dikes and sills. To the north-east from this **central volcanic belt** there are two east-west trending layered volcanic packages, terminated by granitoid bodies in the west. Metasediments are present in the north-eastern part of the AOI, as well as on the south-western side of the central volcanic belt – as a part of the Thunder Lake syncline complex.

The **central volcanic belt** is the most obvious feature in the AOI. Rock samples gathered from the area suggest that this comprises primarily mafic rocks interbedded with felsic volcanics; the strong magnetic banding is very likely caused by gabbro and/or dolerite layers (dikes/sills). **Weakly magnetic felsic sequences** interbedded in between the strongly magnetic mafic/ultramafic layers are known to include volcanics but most importantly also (granitic) **pegmatite bodies**.

Pegmatites are thought to be linked to the **Ghost Lake batholith** (Clark 2009) which is located in the north-western part of the AOI and apparently also to two other smaller granitoid bodies in the area. The first granitoid body is interpreted beneath Mavis Lake and another one near the south-eastern corner of the AOI. These granitoid bodies are possible sources of the lithium bearing fluids that form pegmatites, and so structures that could potentially channel those fluids are of particular interest.

The previous interpretation for Pioneer Resources (Wallace 2018), discussed the possibility of a granitoid body under Mavis Lake. Based on the analysis of airborne data covering a larger area including responses of other granitoid bodies, the existence of the granitoid body under Mavis appears to be almost certain.

In a regional sense, the east-west trend of volcanic belts seems to be dominant over the Mavis Lake AOI. Another prominent structural trend is in the north-east direction, cross-cutting and controlling folding of the central volcanic belt. Major faults have been interpreted in this direction. The axis of the Thunder Lake syncline as well as the western contacts of two smaller granitoid bodies (Mavis Lake and south-eastern granitoids) are also parallel with this direction. These two principal regional directions are very clearly observed in VLF data which were beneficial in structural interpretation.

At the detail scale, volcanic belts are cross-cut and fragmented by (likely brittle) fractures and faults in both diagonal (north-west and north-east) directions, apparently in association with folding processes and granitoid body emplacement pressures. Pegmatites are found to be oriented parallel with volcanic belt foliation, however, some pegmatite occurrences seem aligned with cross-cutting structures.

All granitoid bodies as well as metasediments on the north have their own fracture system.

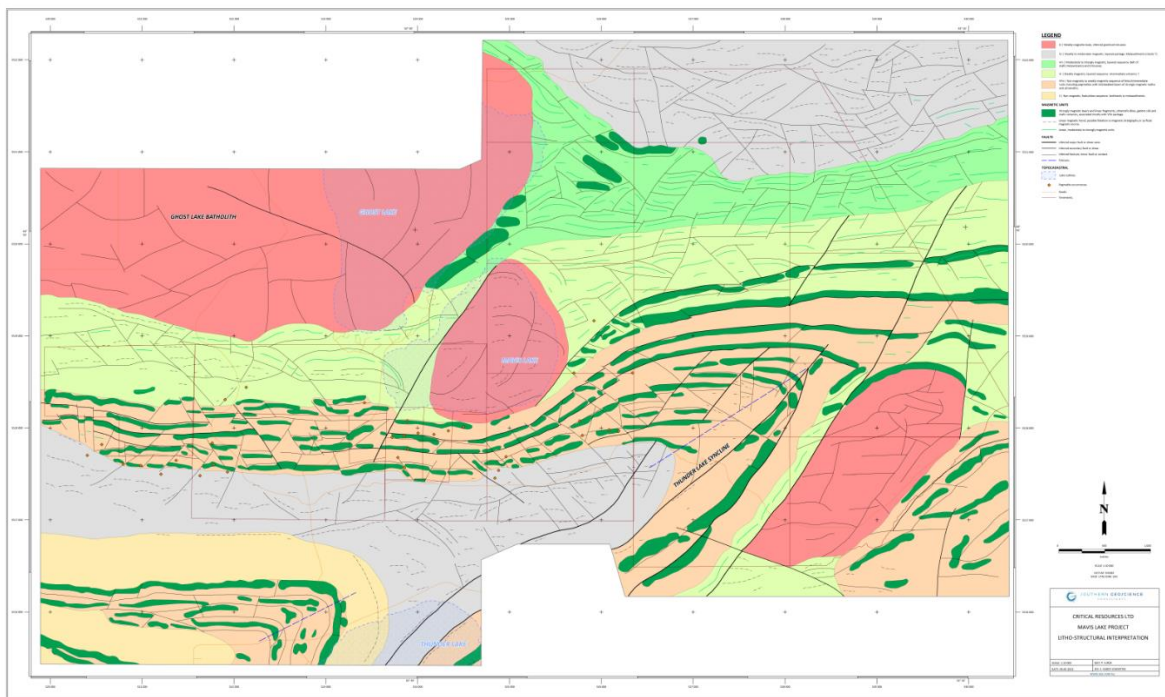


Figure 6: Litho-structural interpretation of Mavis Lake project area.

4.3 Targeting

The targeting process uses the outcome of the litho-structural interpretation of geophysical and other supportive data with particular focus on the following:

- Identification of granitoid intrusions in the area as a possible source of pegmatites with definition of their prospective margins.
- Interpretation of key structural features, such as shear zones, faults, bends, jogs and potential dilational settings.
- Attention paid to distinct magnetic lows within volcanic belts which might indicate felsic lithology consistent with the presence of pegmatites.
- Correlating Li-Be-Ta-Cs geochemical anomalism and known pegmatite and lithium occurrences with favourable litho-structural settings.

The direct identification of pegmatites is not possible using airborne geophysical data alone as pegmatites have no specific magnetic signature and the usefulness of radiometric acquired over the AOI is questionable (as discussed in Chapter 3). The lack of significant correlation between radiometric readings and known pegmatite occurrences is demonstrated in Figure 7.

Targeting for pegmatites must rely on *indirect* leads from structural and lithological interpretation which helps to create better and more detail geological understanding of the area. Using this approach, targeting in the search for pegmatites is helped by elimination of areas where pegmatites are NOT likely present (strongly magnetic mafic units etc) and by suggesting possible areas which do not have any significant magnetic signature. For this purpose, distinct magnetic lows as areas proposed where to look for pegmatites have been outlined and presented in a separate GIS layer.

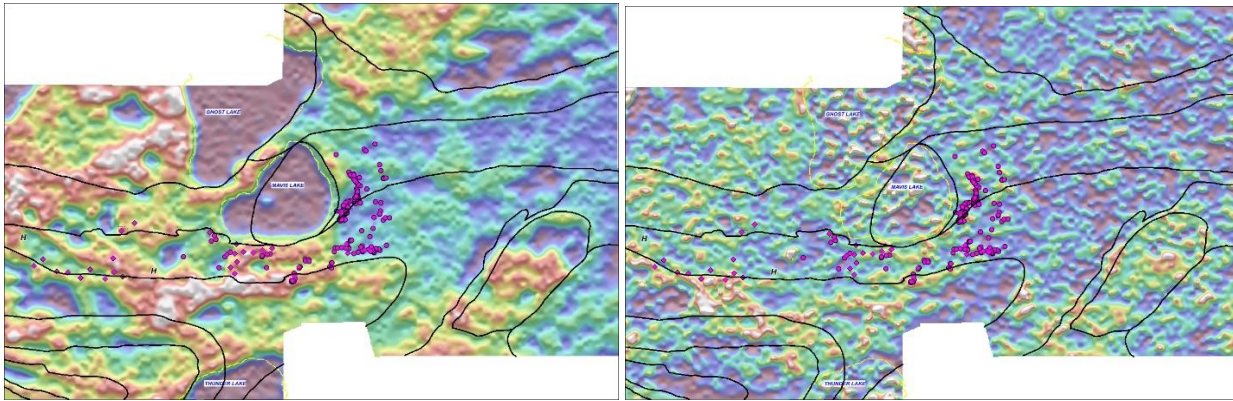


Figure 7: Radiometric potassium concentration image (LEFT) and potassium/thorium ratio image (RIGHT) with basic lithological boundaries (black polygons) and known pegmatite occurrences (magenta symbols) in the overlay. There is no significant correlation between pegmatite occurrences and radiometric anomalies or lithological blocks (except maybe for granites).

The targeting criteria developed for the area is concerned primarily with the following, given in order of importance:

1. Intrusive bodies - proximity to granitoid bodies as likely pegmatite sources.
2. Proximity to prominent structural features such as faults or shear zones or fault bounded alteration and mineralisation.
3. Association with known pegmatite occurrences.
4. Lithological association – in the neighbourhood of mafic complexes indicated by strong magnetic signature.
5. Zones of major tectonic deformation – especially when associated with lithological contacts.
6. Sites of significant structural complexity – intersections, fault terminations, fragmentations etc.

Based on the criteria above, a total of 28 target areas are proposed at Mavis Lake project area. Prioritization of targets is not an easy task with many places seeming to be equally prospective. There is not much difference between priority 1 and 2 targets. Target descriptions are listed below.

Table 2: List of target areas

ID	Priority	Description
1	1	Area along prominent fault, including greatest number of pegmatite occurrences, in close vicinity of granitoid intrusion.
2	1	Area in contact with granitoid body, including number of pegmatite occurrences and distinct magnetic low possibly associated with felsic/pegmatite lithology.
3	1	Structurally complex area with strong fragmentation of magnetic units due to bending of the Vfm sequence. Includes significant number of pegmatite occurrences and magnetic lows possibly indicating felsic/pegmatite lithology.
4	1	Area of widening of Vfm sequence, where two parallel linear magnetic units split into three and more units. Includes distinct magnetic lows and significant number of pegmatite occurrences.
5	1	Area around the prominent strike-slip fault, with signs of alteration.
6	1	Highly deformed area along major fault, including also fold axis.
7	1	Tectonically disturbed area with dislocated and rotated magnetic units around the granitoid contact. Favourable setting for pegmatite formation.
8	1	Complex contact area of granitoid, Vi, and Vfm sequences, includes significant number of pegmatite occurrences.
9	1	Area of fragmentation of Vi sequence because of its bending, in close proximity of granitoid intrusion, includes significant number of pegmatite occurrences.
10	1	Important contact zone of volcanic sequence interrupted by inferred granitoid intrusion. Strong deformation and fracturing suggest favourable setting for pegmatite formation.
11	1	Group of strongly magnetic bodies at the bended contact with granitoid body. Lithological contact and strong deformation around the contact, favourable setting for pegmatite formation.
12	2	Group of magnetic bodies around magnetically quiet area which might indicate felsic lithology including pegmatites. In proximity to granitoid body on the west.
13	2	Area around prominent NE trending fault. Some significant magnetic lows may indicate felsic lithology.
14	2	Area around major fault. Wide gap between magnetic mafic sequences here likely indicates thick sequence of felsic rocks, possibly including pegmatites.
15	2	Series of magnetic lows between two prominent faults in the vicinity of the granitoid body.
16	2	Area of fragmentation of magnetic units, including some significant magnetic lows.

17	2	Tectonically disturbed area with fractures in different directions, having relatively larger non-magnetic section in its centre, possibly indicating felsic lithology including pegmatites.
18	2	Area along distinct fault which is cross-cutting and offsetting sequence of magnetic units.
19	2	Heavily deformed area with fragmented magnetic units, includes some pegmatite occurrences. Coincides with potassium high.
20	2	Number of pegmatite occurrences aligned along NW trending structure.
21	3	Interesting area with series of parallel structures with strike-slip movement.
22	3	Fragmented area which includes number of pegmatite occurrences.
23	3	Magnetic units fragmented and dislocated by cross-cutting structures.
24	3	Significant magnetic low which might indicate felsic lithology including pegmatites.
25	3	Area with some distinct magnetic lows in between magnetic units, possibly indicating felsic/pegmatite lithology.
26	3	Granitoid contact zone, possible pegmatite occurrences associated with magnetic lows.
27	3	Structurally disturbed area with a sharp increase in the number of parallel magnetic units.
28	3	Fragmented area around the fold axis.

5 CONCLUSIONS AND RECOMMENDATIONS

Litho-structural interpretation at a scale of 1:10 000 over the Mavis Lake project area was completed using recently flown magnetic/radiometric/VLF and DEM survey with the help of other supportive data and information from previous exploration efforts. Due to significant forest/forest soil cover over the project area, the structural interpretation was based primarily on the aeromagnetics and to some extent also on VLF data. Radiometric, DEM, satellite data have been studied and analysed, however, these make a minor contribution to the interpretation.

The interpretation was primarily concerned with the identification of pegmatite bodies, prospective for lithium mineralization. With no significant property contrasts between the pegmatites and the typical host rocks, (direct) targeting lithium bearing pegmatites with geophysics is difficult. The targeting strategy was therefore focused on indirect leads: **a)** lithological associations (proximity to granitoid bodies, associations with mafic/ultramafic sequences) **b)** structural context and structural complexity (looking for structures and traps that may act as conduits for Li-bearing fluids to flow and precipitate) **c)** reduction of the search area by eliminating strongly magnetic sequences and looking for distinct magnetic lows, consistent with presumed felsic lithology. In general, preferred were areas of significant structural deformation/fragmentation that

produce favourable conditions for pegmatite precipitation and formation of structures that may act as fluid conduits.

Data concerning known pegmatite occurrences based on geochemistry and previous drilling were utilized in the development of the targeting strategy.

Based on information derived from the geophysical data, a total of 28 target areas have been selected for follow up. Due to the difficulty of detecting pegmatites directly by geophysical methods, the target areas are rather large without exact defined boundaries.

Follow-up reconnaissance drilling, geochemical sampling and further mapping is recommended to obtain geological information about the bedrock geology and mineralisation in the proposed target areas.

Previous work (Wallace 2018) included a range of recommendations, mainly concerned with detailed ground-based radiometrics and magnetics. The analysis of this new, more detailed airborne survey at 75m line spacing (15m grid cell-size) brought new light into these considerations.

Radiometrics may be effective but only over outcropping rocks as the forest soils will likely mask radiometric responses of bedrock lithology. Most effective would be ground spectrometers with reasonably large (2L) crystals carried in a back-pack (such as systems produced by Nuvia/PicoEnvirotec).

Both for ground radiometric and magnetic methods, the differentiation of pegmatites from mafic rocks could be achieved but separating pegmatites and felsic volcanics could be still uncertain.

The brief analysis of satellite Sentinel-2 data (10m pixel) was carried out, but problems associated with forestation and forest soils are even more severe for the case of remote sensing than is the case of radiometric data. Optical spectrometry might work likely over outcrops, where handheld instruments (such as PIMA or similar) may be used. The use of higher resolution satellite or airborne spectrometry (WV3 or HyMap/Spectir) may be more useful but is likely to be high cost and will only work in areas of outcrop (which is limited).

At the detailed scale, the cost of geophysics must be balanced against the cost of simple exploratory shallow drilling. Other geophysical methods that could work are gravity, galvanic resistivity, induced polarisation, ground probing radar, shallow seismics, and sub-audio magnetotellurics (SAM). Once proven, these could be used to both trace known pegmatites under cover and also to locate additional pegmatites within a pegmatite swarm.

For the above methods to work, there must be some sort of geophysical contrast between the pegmatites and their host rocks even if it is only slight. To establish the existence of such contrasts (or not), it is strongly recommended that physical property testing be carried out on small (15cm) representative samples of core from the pegmatites and the main host rocks. With this information, suitable geophysical approaches could be identified. SGC can do this testing if required.

6 REFERENCES

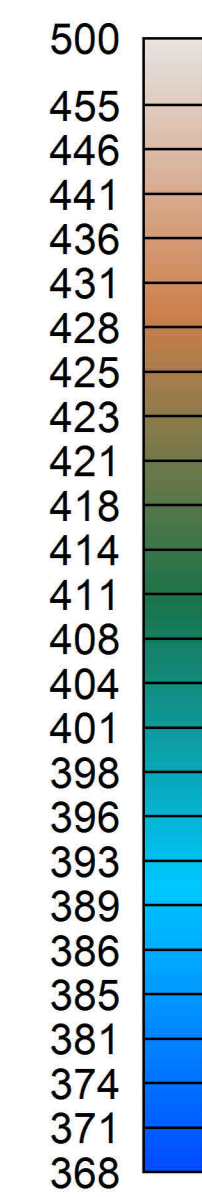
Berlusconi, B., 2000. 1:250,000 Bedrock geology of Ontario. Project GIS Strategy: Building the 250K Precambrian Bedrock geology Theme (PBGT). Report for the Ontario Geological Survey. Map 2115 (Kenora-Fort Frances Sheet) and Map 2065 (Atikokan-Lakehead Sheet) from this compilation were used for geological context.

Clark, J, Breaks, F., Osmani, I., Harrop, J., 2009. Assessment report on the Mavis Lake lithium property, Northwestern Ontario. Prepared for TNR Gold Corp.

Wallace, Y., Trunfull, J., 2018. Raleigh and Mavis Lake projects: Geological Interpretation of Magnetic data for Lithium targets. SGC report 3317 for Pioneer Resources Ltd.

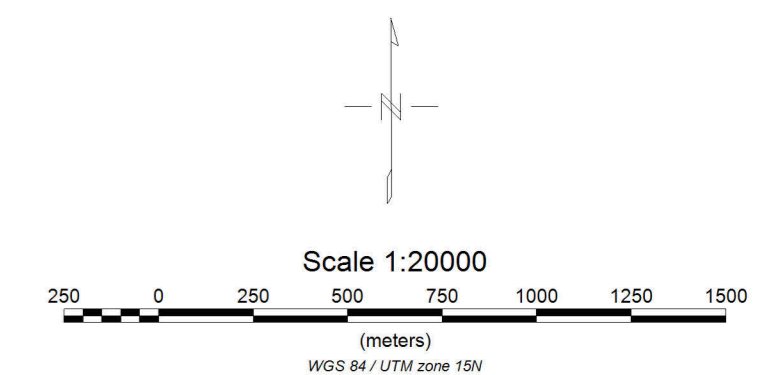
PLANS

PRELIMINARY



World Elevation Model
SRTM 1 arcsec
(meters)

 **Survey Boundary**

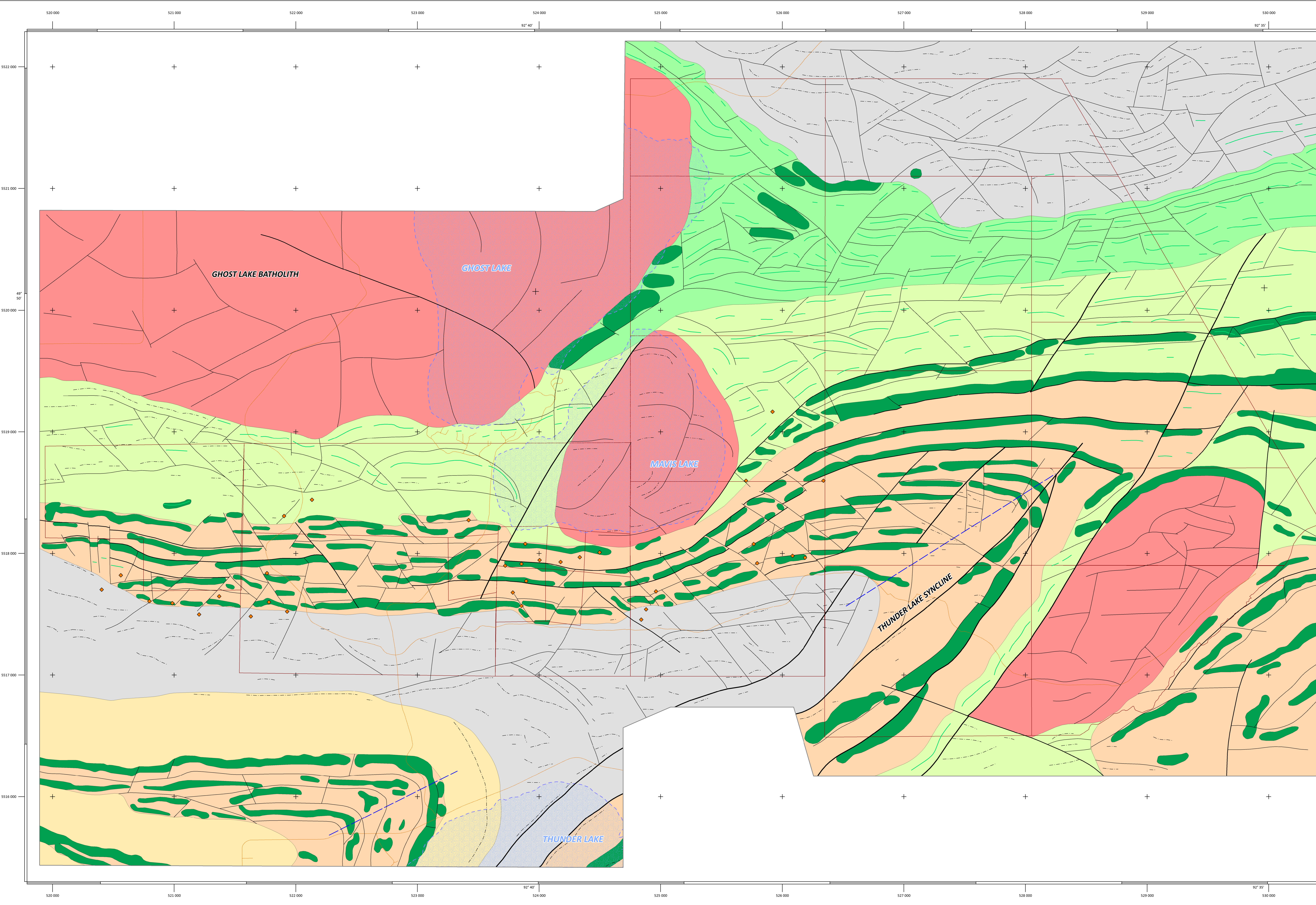


PRELIMINARY

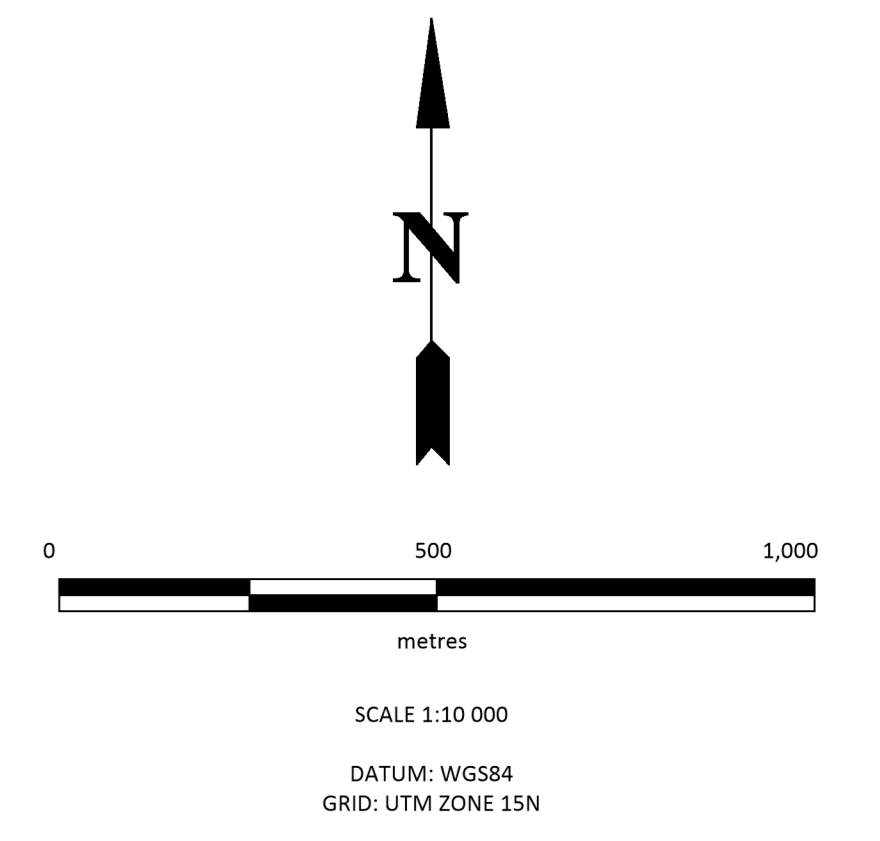
CRITICAL RESOURCES INC.


Preliminary - Flown Flight Path
Up to 2021/11/07

Dryden Block, Ontario
MPX Geophysics Ltd.



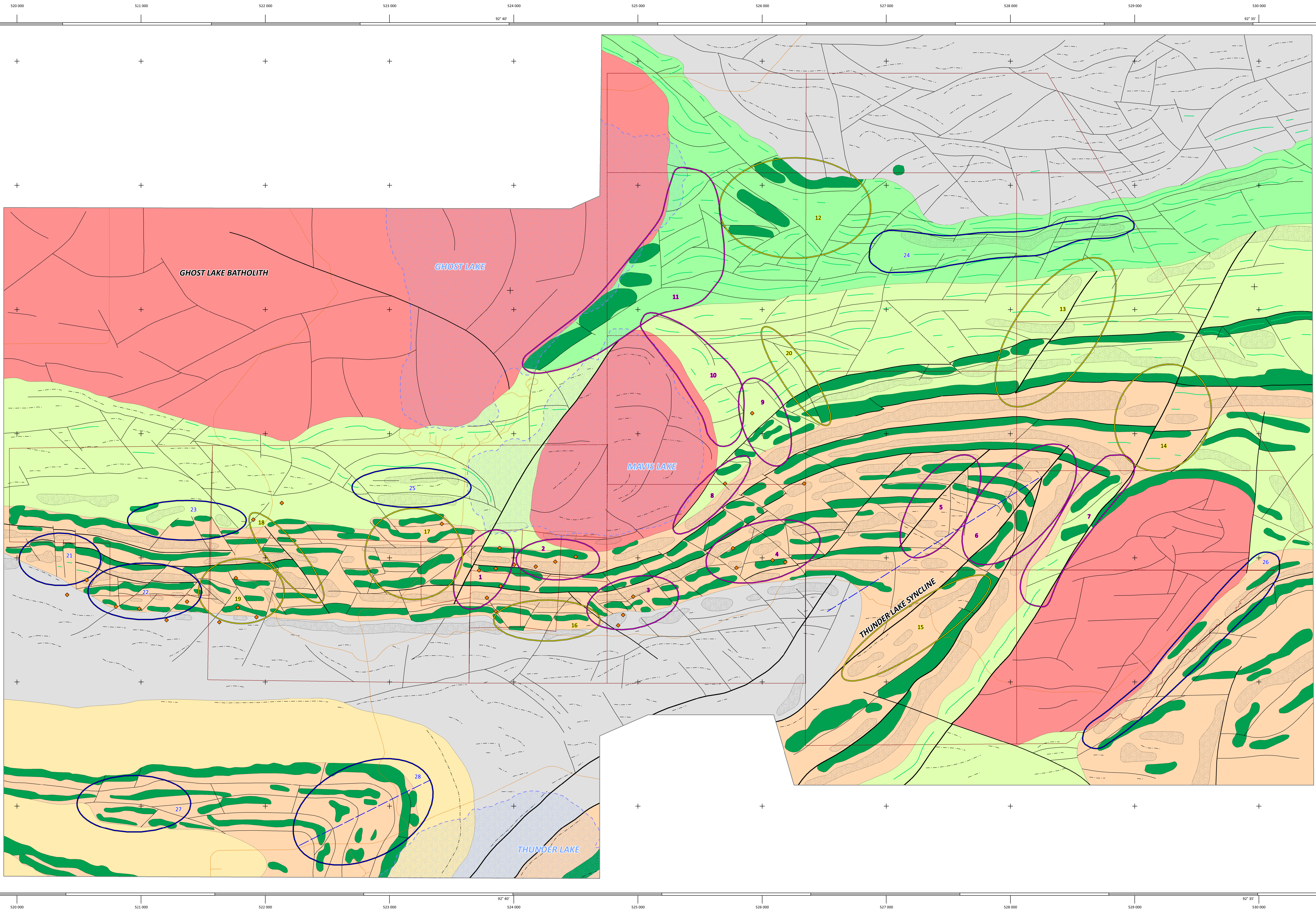
- LEGEND**
- G | Weakly magnetic body, inferred granitoid intrusion.
 - S_c | Weakly to moderately magnetic, layered package. Metasediments (clastic ?).
 - Vm | Moderately to strongly magnetic, layered sequence. Belt of mafic metavolcanics and intrusives.
 - VI | Weakly magnetic, layered sequence. Intermediate volcanics ?
 - Vm1 | Non magnetic to weakly magnetic sequence of felsic/intermediate rocks including pegmatites with interbedded layers of strongly magnetic mafics and ultramafics.
 - S | Non-magnetic, featureless sequence. Sediments or metasediments.
- MAGNETIC UNITS**
- Strongly magnetic layers and linear fragments, ultramafic dikes, gabbro sills and mafic volcanics, associated mostly with Vm package.
 - Linear magnetic trend, possible foliation or magnetic stratigraphy or surficial magnetic source.
 - Linear, moderately to strongly magnetic units.
- FAULTS**
- Inferred major fault or shear zone.
 - Inferred secondary fault or shear.
 - Inferred fracture, minor fault or contact.
 - Fold axis.
- TOPOCADASTRAL**
- Lake outlines.
 - Pegmatite occurrences.
 - Roads.
 - Tenements.



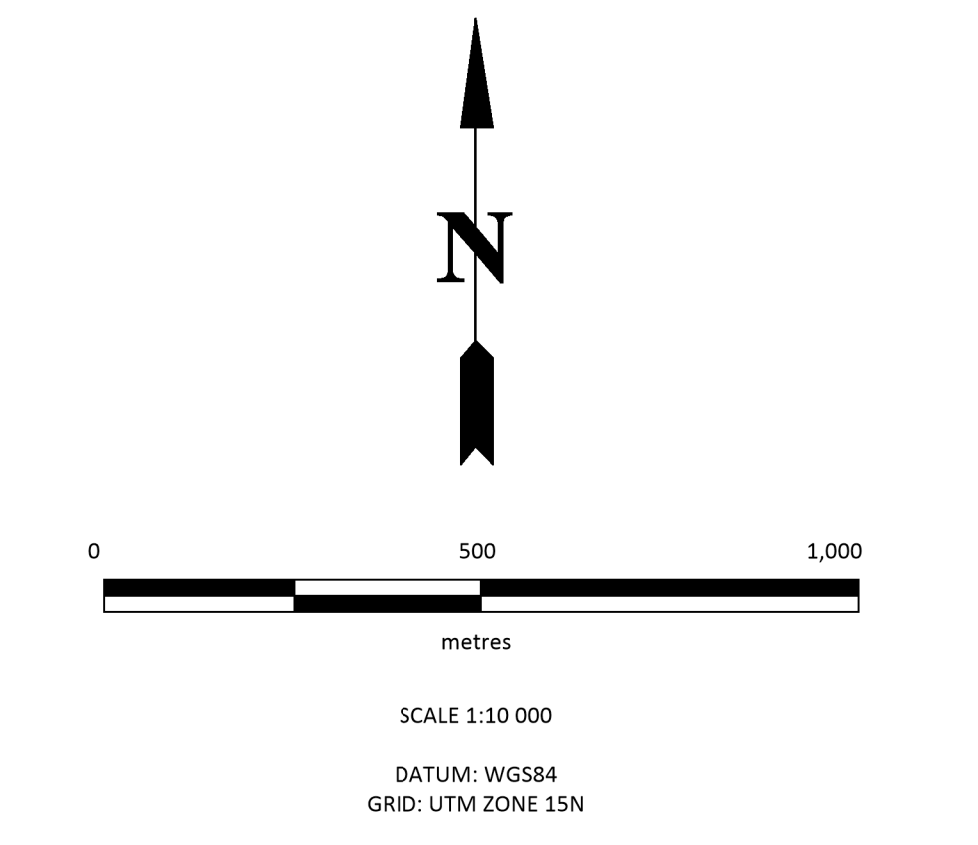

SOUTHERN GEOSCIENCE
 CONSULTANTS

CRITICAL RESOURCES LTD
MAVIS LAKE PROJECT
LITHO-STRUCTURAL INTERPRETATION

SCALE: 1:10 000	GEO: P. JURZA
DATE: 09-05-2022	GIS: S. HARDY-JOHNSTON
WWW.SGC.COM.AU	



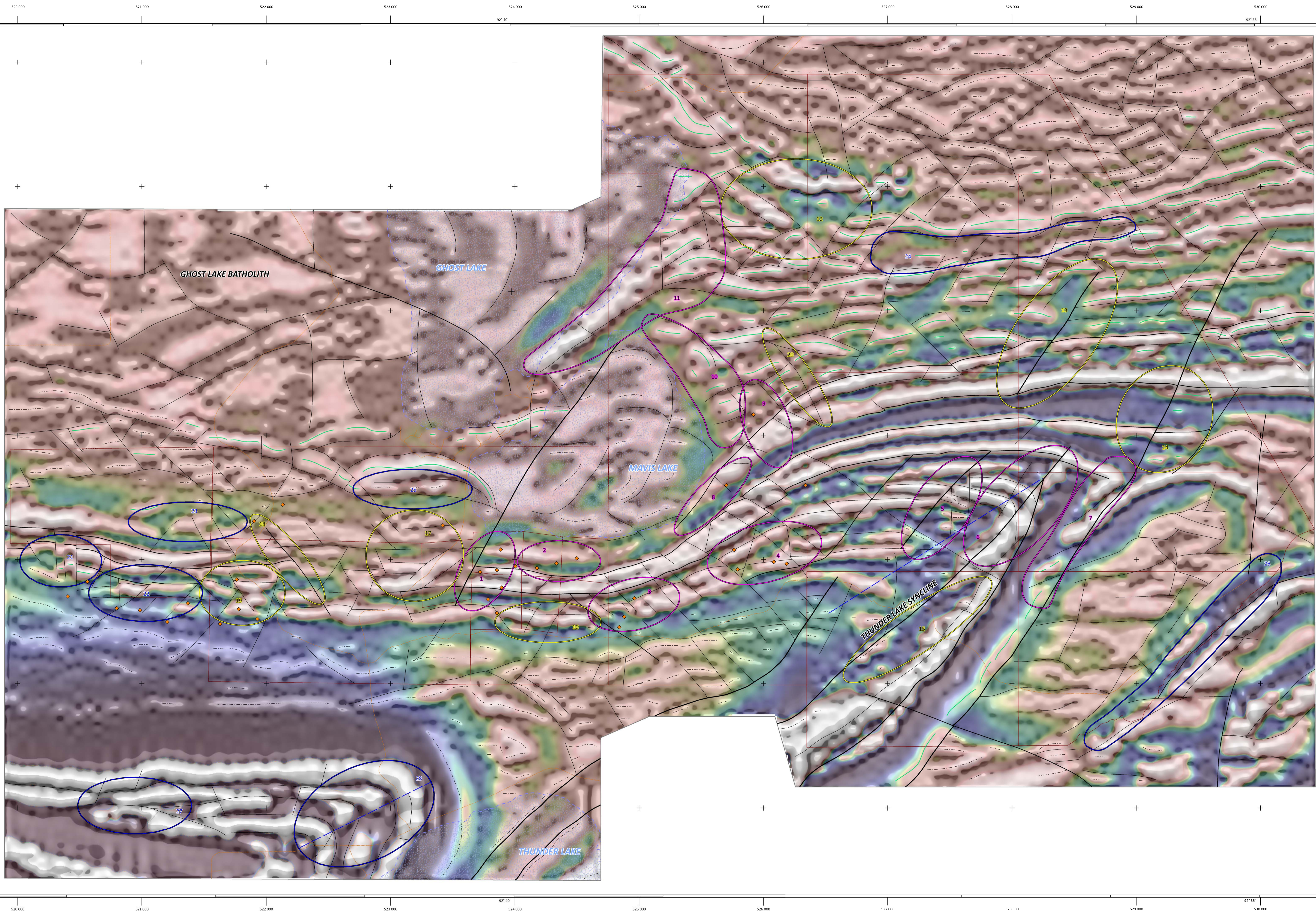
- LEGEND**
- G | Weakly magnetic body, inferred granitoid intrusion.
 - S_c | Weakly to moderately magnetic, layered package. Metasediments (Clastic ?).
 - V_m | Moderately to strongly magnetic, layered sequence. Belt of mafic metavolcanics and intrusives.
 - V_i | Weakly magnetic, layered sequence. Intermediate volcanics ?
 - V_{fm} | Non magnetic to weakly magnetic sequence of felsic/intermediate rocks including pegmatites with interbedded layers of strongly magnetic mafics and ultramafics.
 - S | Non-magnetic, featureless sequence. Sediments or metasediments.
- MAGNETIC UNITS**
- Magnetic lows in between inferred mafic volcanic layers, likely indicating felsic lithology/pegmatites.
 - Strongly magnetic layers and linear fragments, ultramafic dikes, gabbro sills and mafic volcanics, associated mostly with V_{fm} package.
 - Linear magnetic trend, possible foliation or magnetic stratigraphy or surficial magnetic source.
 - Linear, moderately to strongly magnetic units.
- FAULTS**
- Inferred major fault or shear zone.
 - Inferred secondary fault or shear.
 - Inferred fracture, minor fault or contact.
 - Fold axis.
- TOPOCADASTRAL**
- Lake outlines.
 - Pegmatite occurrences.
 - Roads.
 - Tenements.
- TARGETS**
- High priority target
 - Moderate priority target
 - Low priority target



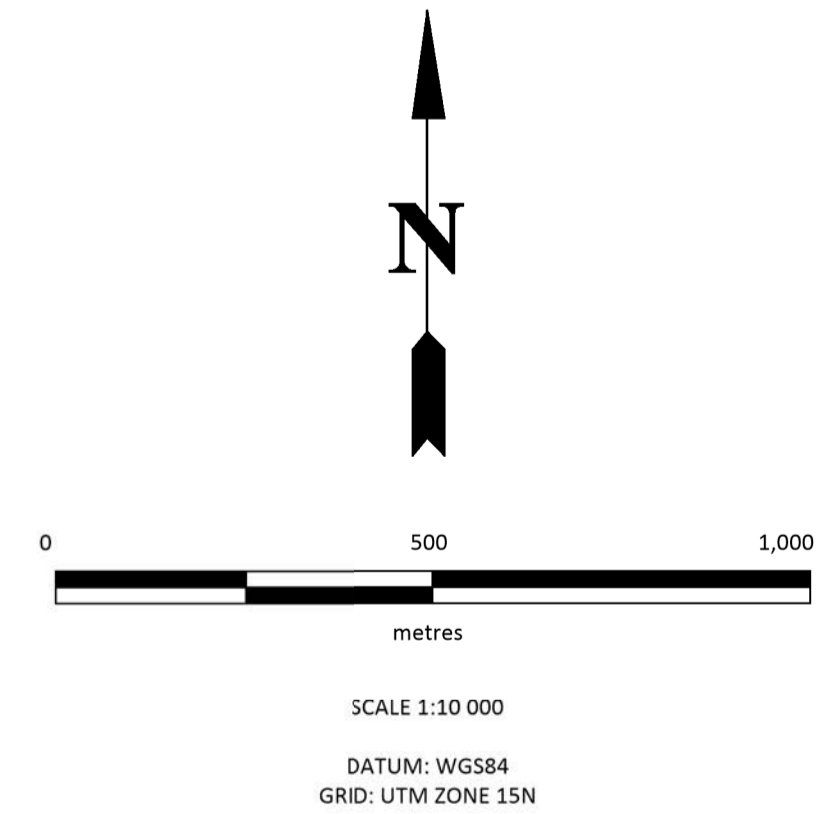
SOUTHERN GEOSCIENCE CONSULTANTS

CRITICAL RESOURCES LTD
MAVIS LAKE PROJECT
LITHO-STRUCTURAL INTERPRETATION
WITH TARGETS

SCALE: 1:10 000	GEO: P. JURZA
DATE: 09-05-2022	GIS: S. HARDY-JOHNSTON
WWW.SGC.COM.AU	



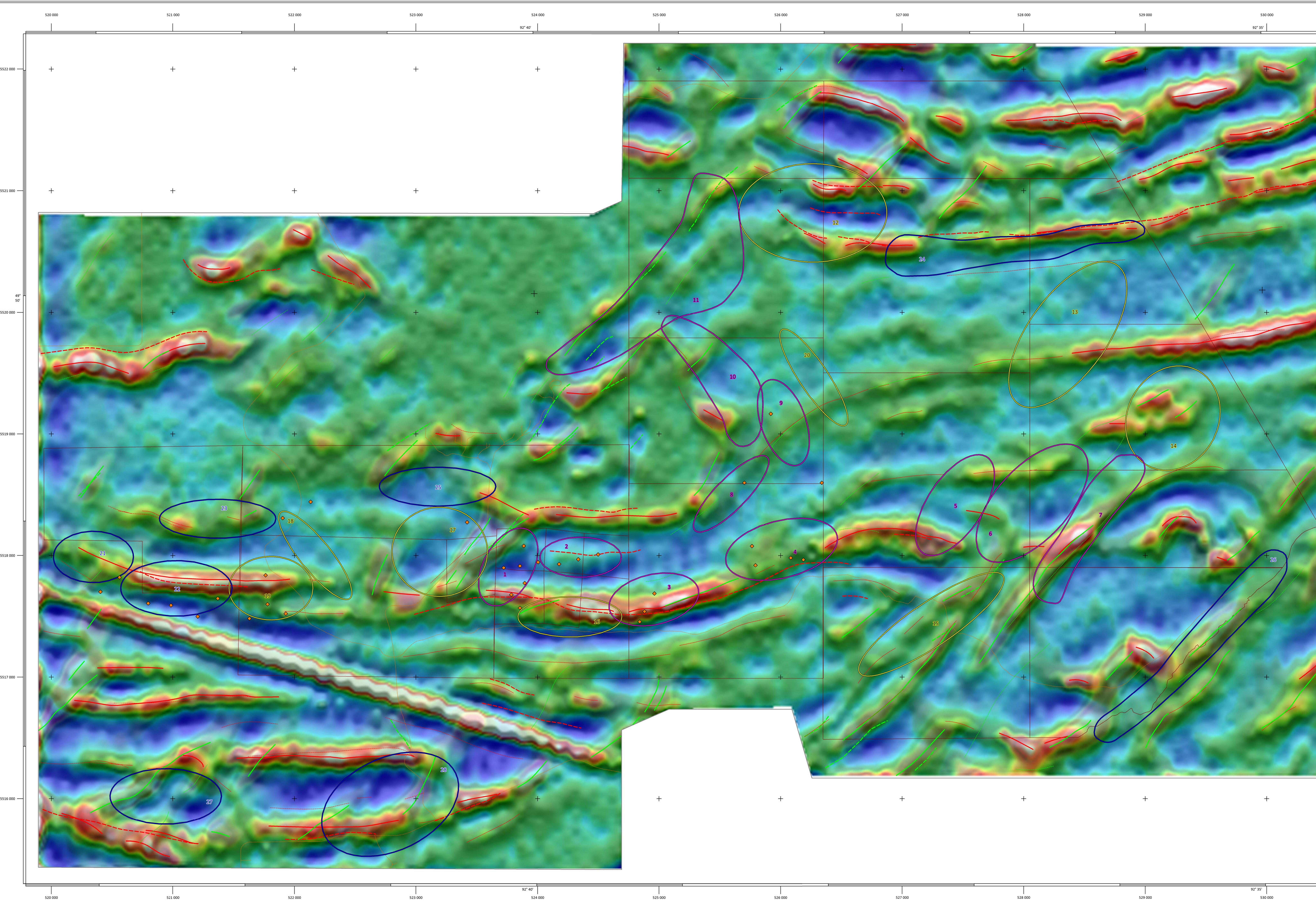
- LEGEND**
- MAGNETIC UNITS**
- Linear magnetic trend, possible foliation or magnetic stratigraphy or surficial magnetic source.
 - Linear, moderately to strongly magnetic units.
- FAULTS**
- Inferred major fault or shear zone.
 - Inferred secondary fault or shear.
 - Inferred fracture, minor fault or contact.
 - Fold axis.
- TOPOCADASTRAL**
- Lake outlines.
 - Pegmatite occurrences.
 - Roads.
 - Tenements.
- TARGETS**
- High priority target
 - Moderate priority target
 - Low priority target



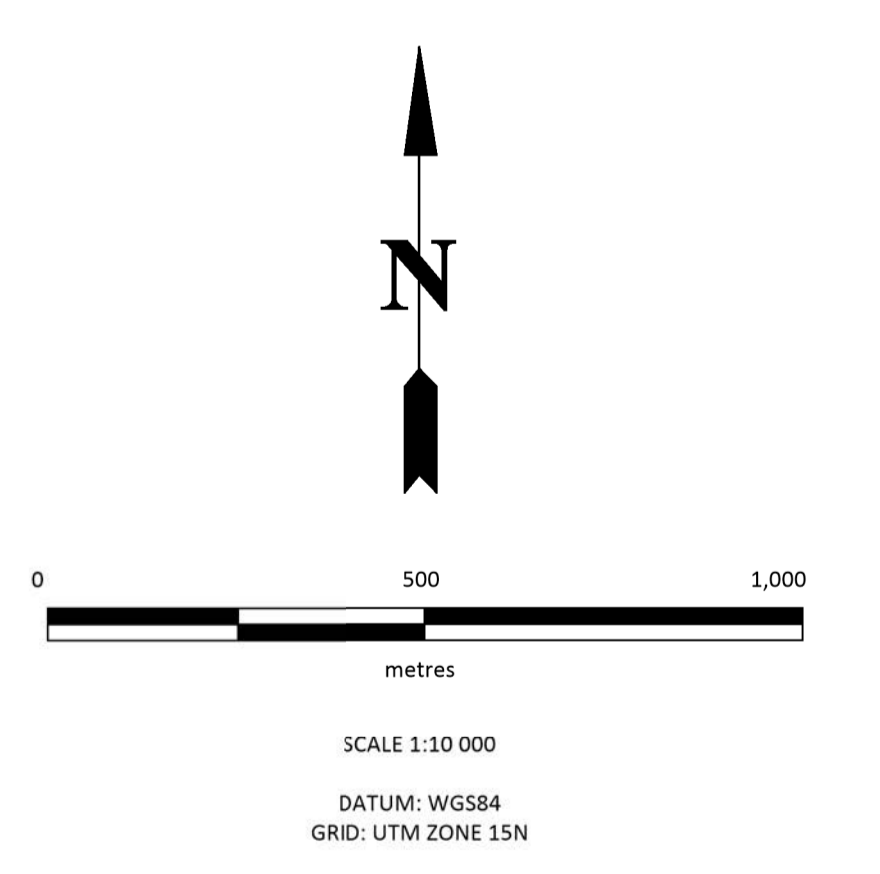
SOUTHERN GEOSCIENCE CONSULTANTS

CRITICAL RESOURCES LTD
MAVIS LAKE PROJECT
STRUCTURAL INTERPRETATION
OVER MAGNETIC IMAGES
(RTP1VD-colour, RTP2VD-pattern)

SCALE: 1:10 000	GEO: P. JURZA
DATE: 09-05-2022	GIS: S. HARDY-JOHNSTON
WWW.SGC.COM.AU	



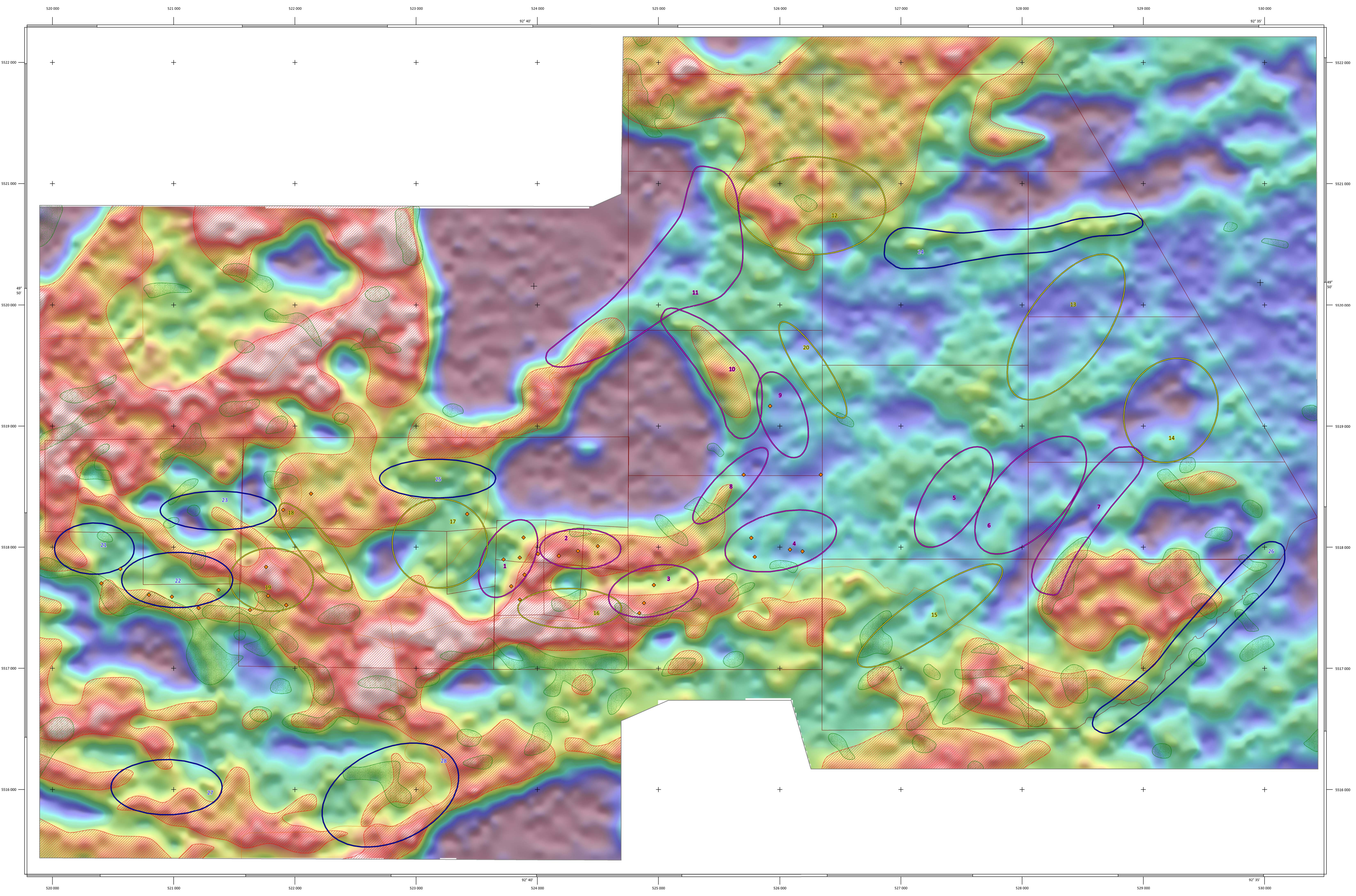
- LEGEND**
- Major total field (line)
 - Minor total field (line)
 - Major total field (ortho)
 - Minor total field (ortho)
 - Major Quadrature (line)
 - Minor Quadrature (line)
 - Major Quadrature (ortho)
 - Minor Quadrature (ortho)
- TOPOCADASTRAL**
- Pegmatite occurrences.
 - Roads.
 - Tenements.
- TARGETS**
- High priority target
 - Moderate priority target
 - Low priority target



SOUTHERN GEOSCIENCE CONSULTANTS

CRITICAL RESOURCES LTD
MAVIS LAKE PROJECT
VLF CONDUCTIVE AXES OVER
VLF TOTAL FIELD-DERIVATIVE IMAGE
(Blend of LINE and ORTHO component)

SCALE: 1:10 000	GEO: P. JURZA
DATE: 09-05-2022	GIS: S. HARDY-JOHNSTON
www.sgc.com.au	



LEGEND

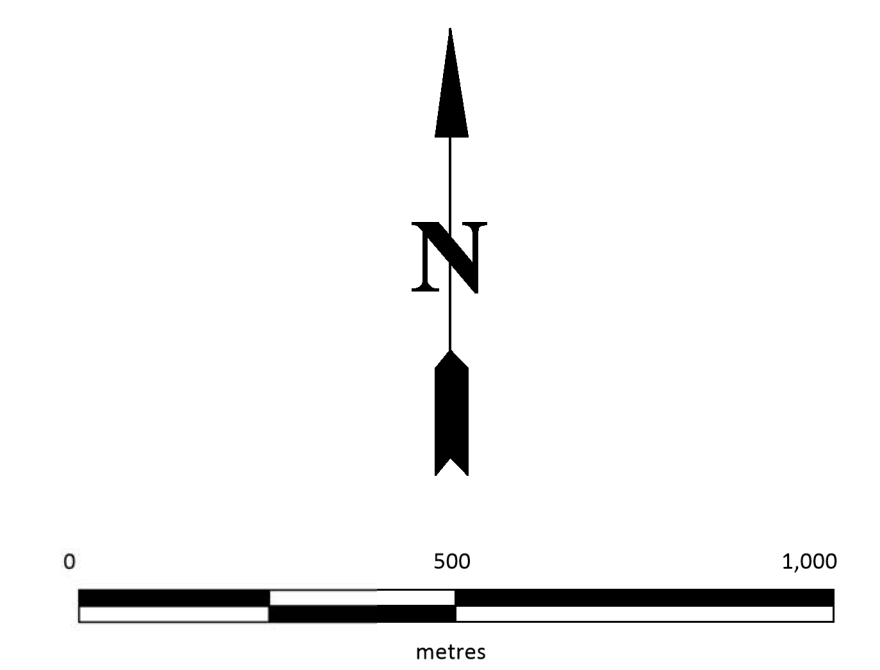
- Potassium concentration anomalies
- Potassium to Thorium ratio anomalies.

TOPOCADASTRAL

- Pegmatite occurrences.
- Roads.
- Tenements.

TARGETS

- High priority target
- Moderate priority target
- Low priority target



SCALE: 1:10 000
 DATUM: WGS84
 GRID: UTM ZONE 15N

SOUTHERN GEOSCIENCE CONSULTANTS	
CRITICAL RESOURCES LTD MAVIS LAKE PROJECT TARGETS AND RADIOMETRIC ANOMALIES OVER POTASSIUM IMAGE	
SCALE: 1:10 000	GEO: P. JURZA
DATE: 09-05-2022	GIS: S. HARDY-JOHNSTON
WWW.SGC.COM.AU	

APPENDIX A:
MPX Survey Details



MPX
GEOPHYSICS LTD.

FINAL

November 2021

CRITICAL RESOURCES LIMITED

45 Ventnor Avenue, West Perth,
WA 6005, Australia.

**Dryden Block - Fixed Wing Airborne
Magnetic/Radiometric/VLF Geophysical
Survey**

Prepared by MPX Geophysics Ltd.

*4-355 Harry Walker Parkway North, Newmarket, Ontario, L3Y
7B3, Canada.*

Ontario, Canada



Tel: (905) 947-1782 **E-Mail:** info@mpxgeo.com
Web: www.mpxgeo.com

Table of Contents i

List of Figures..... iii

List of Tables iii

1.0 Summary..... 4

2.0 Survey Area 5

 2.1 Geophysical Survey 6

3.0 Survey Operations 8

 3.1 Operations Base 8

 3.2 Navigation..... 8

 3.3 Field Processing & Quality Control..... 9

 3.4 Project Status Report..... 9

 3.5 Aircraft..... 10

 3.6 Survey Equipment..... 10

 3.6.1 Survey System Overview..... 10

 3.6.2 Airborne Gamma-ray Spectrometer System..... 11

 3.6.3 Airborne Magnetometer..... 11

 3.6.4 Radar Altimeter..... 12

 3.6.5 Barometric Altimeter 12

 3.6.6 GPS Navigation System..... 12

 3.6.7 Base Station Magnetometer 12

 3.6.8 PC-based Data Acquisition System 13

 3.6.9 Very Low Frequency (VLF) System 13

 3.6.10 Spares 14

4.0 Instrument Checks and Calibrations 15

 4.1 Gamma-ray Spectrometer Checks 15

 4.1.1 Stripping Ratio, Spectrometer Sensitivities, and Altitude Attenuation Coefficients 15

 4.1.2 Cosmic Windows Calibration 15

 4.2 Magnetometer Checks 16

 4.2.1 Manoeuvre noise (Figure of Merit)..... 16

 4.2.2 LAG test (parallax) 17

 4.2.3 Magnetic Heading Effect 17

 4.2.4 Altimeter test – Radar/Barometric/DGPS..... 18

 4.3 VLF Checks 20

 4.3.1 VLF System Coupling 20

 4.3.2 Schedules of the Transmitter Stations..... 21

5.0 Quality Control and Data Processing 22

 5.1 In-Field Processing and Deliverables 22

 5.1.1 Flight Path Compilation..... 22

 5.1.2 Digital Terrain Model 22

 5.1.3 Base Station Magnetic Data..... 22

 5.2 Airborne Magnetic Data 22

 5.2.1 Corrections..... 22

 5.2.2 Gridding 23

5.2.3	Filter Derivatives	23
5.3	Airborne Radiometric Data.....	24
5.3.1	Background for Corrections and Processing.....	24
5.3.2	Processing Applied Using the Geosoft Oasis Montaj Radiometric Processing System 26	
5.4	Airborne VLF data.....	28
5.4.1	Polarity Compensation.....	28
5.4.2	Correction of Time Variations	28
5.4.3	Parallax Correction (LAG)	28
5.4.4	Micro-leveling.....	28
5.4.5	Conversion into percentage values	28
6.0	Deliverable Products.....	29
6.1	Digital Data.....	29
6.1.1	Metadata Files.....	30
6.2	Report.....	30
6.2.1	Statement of Qualifications.....	30
	Appendix 1. Statement of Qualifications	32
	Appendix 2. Digital File Metadata	34
	Appendix 3. Project Status Report.....	38

List of Figures

Figure 1: The Piper Navajo PA31 Registration C-GQVP –aircraft used for the current survey.	4
Figure 2: Survey area location map (red polygon: survey area).	5
Figure 3: Flown flight path map over the Dryden Block.	6
Figure 4: The GEM GSM-19 base-station magnetometer.	8
Figure 5: Piper Navajo PA31 with registration C-GQVP flown during the survey.	10
Figure 6: Scintrex CS-3 Cesium Magnetometer.	12
Figure 7: LAG test result.	17
Figure 8: Cloverleaf flown during the Heading test.	18
Figure 9: Results of the Radar/Barometric/DGPS altimeter test. Correlation coefficient in (A) = 0.9999; correlation coefficient in (B) = 0.9999.	19
Figure 10: Typical airborne gamma-ray spectrum showing the positions of the conventional energy windows.	26

List of Tables

Table 1: Description of survey areas and flown distance.	6
Table 2: Boundary Coordinates of the Survey Block (Datum and Projections are noted)	7
Table 3: QA/QC survey specifications.	9
Table 4: System component sampling rates.	11
Table 5: Sample Regions of Interest (ROI).	11
Table 6: Stripping Ratios.	15
Table 7: Altitude attenuation coefficients and spectrometer sensitivities used in the current project.	15
Table 8: The results of the Cosmic Window calibrations.	16
Table 9: Figure of Merit (FOM) / Maneuver test.	16
Table 10: Results of the flown heading test.	17
Table 11: Altimeter test measured values.	20
Table 12: Base-station magnetic datum.	23
Table 13: IGRF calculation parameters.	23
Table 14: RTP calculation parameters.	24
Table 15: File names and descriptions for all digital data prepared.	34
Table 16: Project Status Report.	38

1.0 Summary

A Fixed wing airborne high resolution magnetic/radiometric/VLF survey was completed over one (1) block identified by the Client as “Dryden”. The work was completed under contract to CRITICAL RESOURCES LIMITED (“the client”).

The MPX equipment was previously installed into the Piper Navajo PA31 (Figure 1) prior to the commencement of the survey campaign in Ontario. The MPX crew arrived in Dryden (Ontario, Canada) on November 5th, 2021, from where the acquisition operations were conducted. The first production flight was completed on November 6th, 2021, and the final survey flight one day after on November 7th, 2021.

A total of 895.6 line-km of data were collected over the Dryden Block. The survey was flown with the best effort to sustain a nominal mean terrain clearance of 70 m along N-S traverse lines separated by 75 m, and E-W control lines at 750 m. All the details of the project areas are summarized in Table 1.

Geophysical data acquisition involved the use of precision differential GPS positioning, a Radiation Solution RSX-5 multi-channel gamma-ray spectrometer system, a high sensitivity magnetometer installed in a tail-stinger and a VLF Totem-2A system. The Piper Navajo Registration C-GQVP was used for this survey.

This report describes the data acquisition and processing procedures, parameters, and delivery products for this survey.



Figure 1: The Piper Navajo PA31 Registration C-GQVP –aircraft used for the current survey.

2.0 Survey Area

A fixed-wing borne high resolution magnetic/radiometric/VLF survey was completed over the one (1) block identified by the Client as Dryden Block, as illustrated in Figure 2 Figure 3.

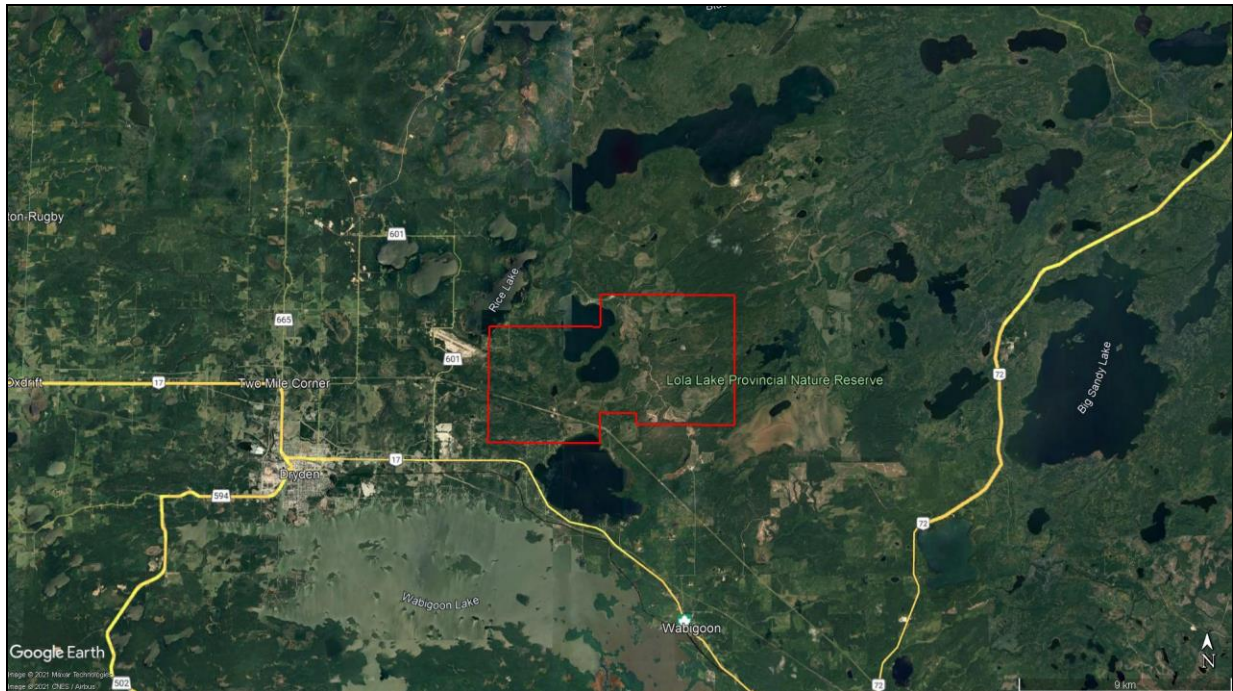


Figure 2: Survey area location map (red polygon: survey area).

The topography in the survey area was relatively smooth and the change in elevation was approximately from 360 m to 500 m in Dryden area. During production the weather conditions were typically mild to warm (+5°C to +25°C) with light to moderate winds.

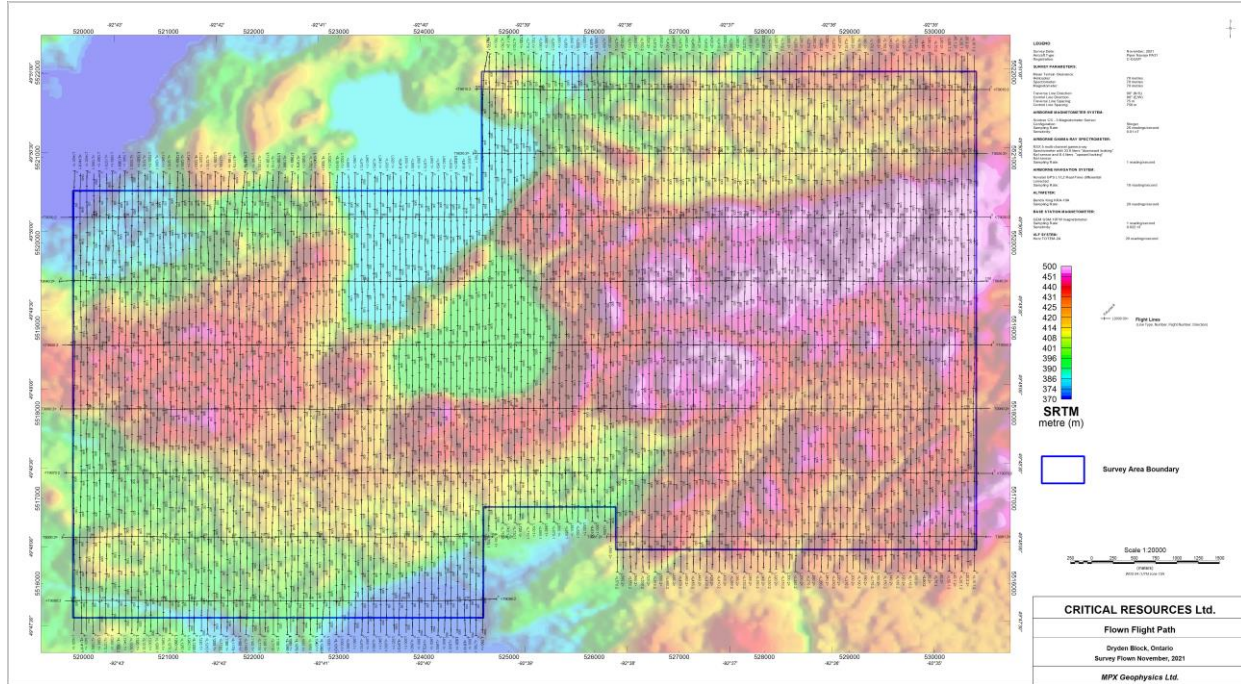


Figure 3: Flown flight path map over the Dryden Block.

2.1 Geophysical Survey

The Project Area was flown according to client requirements, while considering the topographical conditions and needed spatial resolution. The details of the flown area are summarized in Table 1.

Table 1: Description of survey areas and flown distance.

Block Name	Nominal Altitude (AGL)	Traverse Lines			Control Lines			Total line-km	Area (km ²)
		Direction	Spacing	Line-km	Direction	Spacing	Line-km		
Dryden	70 m	N-S (0°)	75 m	814.0	E-W (90°)	750 m	81.6	895.6	55.88

The survey block corner coordinates were requested in WGS84, Zone 15N UTM easting and northing. These are provided below in Table 2.

Table 2: Boundary Coordinates of the Survey Block (Datum and Projections are noted)

DRYDEN BLOCK				
WGS84				
UTM Zone 15N			Geographic Coordinates	
Corner	X - Easting	Y - Northing	Longitude	Latitude
1	519880	5520610	92° 43' 24.7306" W	49° 50' 15.3200" N
2	524680	5520610	92° 39' 24.4282" W	49° 50' 14.6776" N
3	524680	5522010	92° 39' 24.1072" W	49° 51' 00.0081" N
4	530490	5522010	92° 34' 33.1693" W	49° 50' 59.0451" N
5	530490	5516400	92° 34' 34.7565" W	49° 47' 57.4006" N
6	526255	5516400	92° 38' 06.6049" W	49° 47' 58.1213" N
7	526255	5516900	92° 38' 06.4832" W	49° 48' 14.3109" N
8	524700	5516900	92° 39' 24.2771" W	49° 48' 14.5485" N
9	524700	5515600	92° 39' 24.5746" W	49° 47' 32.4556" N
10	519880	5515600	92° 43' 25.6543" W	49° 47' 33.0999" N

3.0 Survey Operations

3.1 Operations Base

Survey operations were based in Dryden (Ontario, Canada) during this program. One magnetic base station was used during the project (Figure 4).



Figure 4: The GEM GSM-19 base-station magnetometer.

The station was positioned to minimize the distance to the survey block, and/or to provide a back-up data set.

Quality Control and preliminary data processing was undertaken by the crew in the field and in office as the survey progressed.

3.2 Navigation

The nominal data acquisition speed of the aircraft was slower than 280 km/h (78 m/s – 150 knots). Magnetic, VLF and radar altimeter data were sampled 20 times per second (20 Hz). The GPS position was sampled ten times per second (10 Hz), and the spectrometer data at 1 Hz. A position fix was recorded approximately every 7.8 m along the flight track. Magnetometer, VLF and radar altimeter data measured every 0.05 s, collected about every 3.9 m along the survey line, and radiometric samples every 78 m.

Navigation was assisted by a Novatel L1/L2 GPS system that reported GPS coordinates as WGS84 latitude and longitude and guided the pilot over a pre-programmed two-dimensional (2-D) survey grid. The x-y position of the aircraft registered by the GPS system was recorded with the terrain clearance as reported by the radar altimeter.

Vertical navigation along flight lines was established using a radar altimeter. The nominal terrain clearance consisted of the best effort to follow up the topographic contour at 70 m above ground level. This ground clearance was the same for the aircraft, magnetometer, VLF and spectrometer sensors.

3.3 Field Processing & Quality Control

The survey data were transferred to portable recording media on a flight-by-flight basis, and subsequently copied to the field data processing workstation. In-field data processing included conversion of the data to GEOSOFT GDB database format and inspection of the data for adherence to contract specifications listed below in Table 3. Survey lines that exhibited excessive deviation, or were considered to be of inferior quality, were re-flown. None of the flight lines required partial or complete re-flight due to equipment malfunction.

Table 3: QA/QC survey specifications.

QA/QC SURVEY SPECIFICATIONS	
DRYDEN BLOCK	
Traverse Lines Direction	N-S (0°)
Traverse Lines Spacing	75 m
Control Lines Direction	E-W (90°)
Control Lines Spacing	750 m
Flight Path Deviation (25% of SL spacing over a distance of more than 1 km)	Best effort to not deviate greater than 19 m over 1000 m
Base-station mag. diurnal	12 nT peak-to-peak over 5 min
Figure of Merit (FOM)	Shall remain below 1.5 nT after compensations
Gamma-ray Spectrometer	Radiometric data to be assessed under awareness of the survey height influence and local weather variations.
Survey Speed	< 150 knots (78 m/s)
Flight Altitude	Best effort to follow up the terrain contour at 70 m AGL, not exceeding +15 m deviation over more than 1 km.

3.4 Project Status Report

The project status report summarizes all information relevant to the project for each day of the survey. Details include the type of activity carried out on each day (mobilization, installation, equipment troubleshooting, production, weather down-day, or pilot day off); the flight numbers; total line-km flown; total flight hours; personnel working; and any additional details for each day. The report also provides a summary of the survey block names and the line-km flown in each. The project status report is included in Appendix 3.

The installation of the geophysical and ancillary equipment was carried out by MPX personnel. The MPX operator was responsible for ensuring that the equipment functioned properly and within specifications, operating the survey equipment during data acquisition, and carrying out preliminary quality control of

the acquired data.

3.5 Aircraft

The survey was flown using a fixed-wing Piper Navajo PA31 with a crew of two pilots on board (Figure 5). The aircraft's details are specified as follows:

Aircraft Registration:	- C-GQVP
Empty weight:	- 1,783 kg (3,930 lbs)
Service ceiling:	- 8,000 m / 26,300 ft (with oxygen)
Survey duration:	- 5.5 hours (no reserves)



Figure 5: Piper Navajo PA31 with registration C-GQVP flown during the survey.

3.6 Survey Equipment

3.6.1 Survey System Overview

The system consisted of a DAARC-500 Data Acquisition System, GPS Novatel L1/L2 navigation, Bendix King radar altimeter, Billingsley Fluxgate Magnetometer, one Scintrex CS-3 high-sensitivity Cesium magnetometer mounted into a fixed tail-stinger, two crystal packs of Radiation Solution RSX-5 multi-channel gamma-ray Spectrometers (256 channels configuration), one VLF Herz TOTEM-2A system, Setra 276 barometric altimeter, and a Honeywell PPT set of temperature and pressure. The sampling rates for each component of the system are presented in Table 4.

Table 4: System component sampling rates.

SYSTEM / No. of CHANNELS	SAMPLING RATES
Total Field Magnetometer (1 channel)	20.0 / sec
Radar Altimeter (1 channel)	20.0 / sec
Billingsley Fluxgate Magnetometer (3 channels)	20.0 / sec
Barometric Altimeter (1 channel)	10.0 / sec
GPS Navigation	10.0 / sec
Gamma-ray Spectrometer (256 channels plus U, Th, K, TC and cosmic)	1.0 / sec
Temperature / Pressure (2 channels)	1.0 / sec
VLF (4 channels – LINE & ORTHO)	20.0 / sec

3.6.2 Airborne Gamma-ray Spectrometer System

Two crystal packs of Radiation Solution RSX-5 multi-channel gamma-ray spectrometers with total 33.6 litres "downward looking" NaI sensor, and 8.4 litres "upward looking" NaI sensor, were installed on the aircraft for the survey. The thermally isolated NaI crystal sensors were installed on a platform mounted inside the fuselage of the airplane. The spectrometers were integrated with the DAARC-500 data acquisition system, and data were sampled once per second.

The downward NaI sensor crystals record the radiometric spectrum from 410 KeV to 3 MeV over 1024 discrete energy windows (Table 5), recorded as photon counts in 1023 equal interval energy channels and one cosmic ray channel that detects photons with energy levels above 3.0 MeV. The RSX-5 is a self-stabilizing spectrometer and tracks and corrects for the spectral drift by following a spectral peak, typically Thorium. The spectral record was then exported in a 256 windows format. The standard Total Count, Potassium, Uranium, Thorium and Cosmic regions of interest were extracted using the window limits listed in Table 5. The upward NaI sensor crystal is used to measure and correct for radon.

Table 5: Sample Regions of Interest (ROI).

Sample of Standard Windows		
Element	Approximate Lower Boundary (MeV)	Approximate Upper Boundary (MeV)
Total Count	0.41	2.81
Potassium	1.37	1.57
Uranium	1.66	1.86
Thorium	2.41	2.81
Cosmic	3.00	∞

Additionally, MPX's procedures are based on the recommendations as described in the International Atomic Energy Agency - IAEA-TECDOC-1363 - Guidelines for radioelement mapping using gamma-ray spectrometry data. A copy of this document is available on request.

3.6.3 Airborne Magnetometer

The magnetic sensor utilized for the survey was a Scintrex CS-3 high resolution cesium split-beam total-

field magnetometer, which was installed in a tail mounted stinger. The sampling rate was twenty (20) times per second with an in-flight sensitivity of 0.002 nanoTesla (nT). Aerodynamic magnetometer noise was +/- 0.01 nT. The sensitivity of the magnetometer was recorded at 0.002 nT when operated at a sampling rate of 0.05 seconds.



Figure 6: Scintrex CS-3 Cesium Magnetometer.

A Cesium vapour magnetic sensor is a miniature atomic absorption unit, producing a signal whose frequency (Larmor frequency) is proportional to the intensity of the ambient magnetic field. The unit consists of three main elements; a Cesium vapour lamp, an absorption cell, and a photosensitive diode.

These components are mounted along a common optical axis within the sensor housing. The electronic support system is mounted in the middle of the forward mounted stinger, transmitting the Larmor signal to a counter in the data acquisition system then converted the signal to magnetic field strength in nanoTeslas.

3.6.4 Radar Altimeter

A Bendix King KRA-10A altimeter recorded the ground clearance distance to an accuracy of +/- 2% over a range of 0 to 2,500 ft.

3.6.5 Barometric Altimeter

A Setra Model 276 Pressure Transducer recorded the barometric pressure to an accuracy of about 1 ft (30 cm). The barometric altimeter was mounted on the DAARC frame inside the fuselage of the aircraft.

The altimeter was interfaced to the data acquisition system with a sample rate of 0.1 seconds, and was digitally recorded.

3.6.6 GPS Navigation System

A Novatel L1/L2 GPS navigation system input to a navigation computer and Pilot Guidance Unit (PGU) provided navigation control. The pilot guidance unit (PGU) provided steering and cross-track guidance to the pilot. The pilot was provided with GPS and altimeter data to assist in the flying of the aircraft.

Survey coordinates were set up prior to the commencement of the survey, and the information was loaded into the airborne navigation system. The GPS positional data was recorded at 10 Hz intervals and used to calculate real-time differentially corrected locations.

3.6.7 Base Station Magnetometer

One GEM Systems GSM-19TW Overhauser magnetometer with onboard GPS was utilized to monitor and record the Earth's magnetic field's diurnal variations. The base station magnetometer was set up at the base of operations for the respective survey area. The magnetic sensor was set up utilizing a staff mount

at the height of 1.7 m above ground. Every effort was made to ensure that the magnetometer sensor was placed in a location with a low magnetic gradient and sited away from electric transmission lines and moving ferrous objects, such as motor vehicles and aircraft, without compromising safety and local activity.

The base-station magnetometer operated continuously throughout the airborne data acquisition work with a sensitivity of 0.022 nT. The ground and airborne system clocks were synchronized using UTC time. The sample rate of the base magnetometer was one time per second (1 Hz). A continuously updated profile plot of the base station values was presented on the base station screen. The magnetometer base station data were recorded in the solid-state memory of the base station and downloaded to the field laptop at the end of each day's survey operations.

3.6.8 PC-based Data Acquisition System

The RMS Automatic Aeromagnetic Digital Compensator (DAARC 500) was used as the magnetometer processor and real-time compensator. Magnetic compensation of the acquired "raw" magnetometer data was collected in real-time using an RMS Instruments DAARC500 Data Acquisition and Aeromagnetic Real-Time Compensator, together with comprehensive and flexible data acquisition and recording. The RMS Instruments' DAARC500 offers the ultimate in aeromagnetic compensation. Powerful, versatile and rugged, yet compact and light, the DAARC500 is ideally suited to airborne geophysical environmental survey applications.

Aeromagnetic compensation in the DAARC500 has its roots in the AADCII, for many years the de facto standard in aeromagnetic compensation in the geophysical exploration industry throughout the world. The result of many years of R&D by RMS Instruments and collaboration with the Flight Research Laboratory of the National Research Council of Canada, the DAARC500 continues the AADCII tradition of consistently producing outstanding data in a cost-effective manner.

The system is built on the foundation of state-of-art, very reliable hardware, firmware, sophisticated and robust compensation algorithms proven in many installations. Consistent with compensation, data acquisitions delivered with unparalleled performance, accuracy, and reliability.

In simple terms, the compensation algorithm will accept the outputs of the cesium magnetometer sensor and orientation sensors and will produce readings of compensated magnetometer data. Using proprietary digital processing techniques, the basic magnetometer processing software can resolve down to 0.0002 nT at twenty samples per second.

The attitude and motion of the aircraft in flight, with respect to the Earth's magnetic field vector, will be monitored/recorded by a three-component fluxgate magnetometer (Billingsley TFM 100G2 Triaxial Fluxgate Magnetometer), which is very sensitive to attitude changes. The outputs of this magnetometer, or motion or attitude sensor, will be used in the mathematical computations of the compensated magnetometer data.

3.6.9 Very Low Frequency (VLF) System

A Herz TOTEM-2A system was installed into the aircraft for measuring the magnetic component of fields radiated from one or two VLF radio transmitters in the 15 to 25 kHz frequency range. These transmitters are located around the world for the purposes of navigation and communication with submarines. The parameters measured are the change in the total field (Hz TOT) relative to the primary field and the vertical quadrature component (Hz QUAD). The sign of the quadrature polarity is also recorded. The system includes a sensor comprising three mutually orthogonal ferrite-cored coils and a pre-amplifier mounted on an assembly, which can be inserted inside an airfoil. It operates in a sensitivity range from

130 $\mu\text{V}/\text{m}$ to 100 mV/m at 20 kHz, and 3 dB down at 14 kHz and 24 kHz.

3.6.10 Spares

A complement of spare parts and test equipment were maintained at the survey site. In addition, MPX kept an equipment log noting all equipment serial numbers, date and time of equipment repair and replacement throughout the survey.

4.0 Instrument Checks and Calibrations

The following airborne magnetometer system tests and calibration checks were completed at appropriate times during the survey.

4.1 Gamma-ray Spectrometer Checks

4.1.1 Stripping Ratio, Spectrometer Sensitivities, and Altitude Attenuation Coefficients

Results from Radiation Solution Spectrometer test and calibration are detailed in Table 6.

Table 6: Stripping Ratios.

Stripping Ratio	Value
Th into U (alpha)	0.27
Th into K (beta)	0.415
U into K (gamma)	0.765
U into Th (a)	0.05
K into Th (b)	Assumed 0
K into U (g)	Assumed 0

Altitude coefficients identify how the radioactive source signature degrades approximately exponentially with increasing distance from the source (i.e. the ground material of interest) and are necessary for equivalent height calculations of radiometric count rates. The altitude attenuation coefficients and spectrometer sensitivities for the MPX RSX-5 spectrometer are summarized in Table 7.

Table 7: Altitude attenuation coefficients and spectrometer sensitivities used in the current project.

Channel	Attenuation Coefficient	Sensitivity
Potassium	-0.0085 cps/m	75.0 cps/%
Uranium	-0.0082 cps/m	7.5 cps/ppm
Thorium	-0.0062 cps/m	4.5 cps/ppm
Total Count	-0.0055 cps/m	23.0 cps/nGy/h

4.1.2 Cosmic Windows Calibration

In each spectral window, the radiation increases exponentially with height due to radiation of cosmic origin, and there is a constant source of background radiation from the aircraft itself. Cosmic window calibrations are carried out to determine background attenuation coefficients for the detector crystal packs. This procedure was performed by flying at various altitudes, each altitude flown for a minimum of 2 minutes.

The average values of the counts measured in each of the 4 windows (TC, U, Th and K) are compared against the average counts for the cosmic window measured at each altitude. The results of the values used for the least-squares fit $N_n = a_n \cos + b_n$ are summarized in Table 8 below (see appendix 5 for more detailed information).

Table 8: The results of the Cosmic Window calibrations.

RESULTS OF LEAST SQUARES FIT TO $N_n = a_n \text{COS} + b_n$ RELATIONSHIP:				
Parameter	TC (cps)	K (cps)	U (cps)	Th (cps)
Cosmic Stripping Ratio Slope (a_n)	0.600	0.032	0.026	0.030
Aircraft Background Intercept (b_n)	90.00	4.00	1.00	1.50

4.2 Magnetometer Checks

4.2.1 Manoeuvre noise (Figure of Merit)

As the magnetic sensor installed in the tail-mounted stinger is still within the magnetic effect of the aircraft structure, tests were conducted to determine the effects of aircraft pitch, roll and yaw. The tests were completed at high altitude over a low magnetic gradient area by carrying out $\pm 5^\circ$ pitches, $\pm 10^\circ$ rolls, and $\pm 5^\circ$ yaw manoeuvres flown over periods of at least 4-5 seconds in the four cardinal directions.

A compensation Figure-of-Merit (FOM) was calculated by summing the peak-to-peak amplitudes of the twelve (12) residual magnetic signatures. The residual magnetic signatures were calculated by applying a high pass filter (with a length of 90 fiducials) to the compensated magnetic data. The amplitudes were then determined from the absolute range of the residual magnetic signature during each pitch, roll, or yaw (peak-to-peak) manoeuvre. The FOM is used as an indicator of performance and should remain below a value of 1.5 nT for the system configuration used in this survey. The compensation box suitable for the Piper Navajo flights was flown with directions 090° , 180° , 270° , 360° (Table 9). The FOM was determined to be 0.63 nT.

Table 9: Figure of Merit (FOM) / Maneuver test.

Pre-Compensation (HP of 90 fids applied to TMI)					
Line	Direction	Pitch	Roll	Yaw	Total
L90	90	0.290	0.6600	0.1100	1.0600
L180	180	0.72	0.6100	0.2800	1.6100
L270	270	0.590	0.4500	0.2500	1.2900
L360	360	0.180	0.4800	0.1000	0.7600
Total		1.7800	2.2000	0.7400	
FOM =		4.7200	nT		

Post-Compensation (HP of 90 fids applied to TMI)					
Line	Direction	Pitch	Roll	Yaw	Total
L90	90	0.080	0.060	0.070	0.210
L180	180	0.050	0.060	0.060	0.170
L270	270	0.040	0.030	0.050	0.120
L360	360	0.060	0.030	0.040	0.130
Total		0.112	0.180	0.174	
FOM =		0.630	nT		

4.2.2 LAG test (parallax)

Since survey lines are often flown alternately in the opposite direction, the electronic delays during recording can result in values being shifted systematically. This test is one possible cause of the so-called "herringbone" effect sometimes seen on contour map of surveys. The test consists in checking these delays by overflying a magnetic object twice in opposite directions.

The resulting LAG value from the test was eight (8) fiducials (0.4 seconds) (Figure 7).

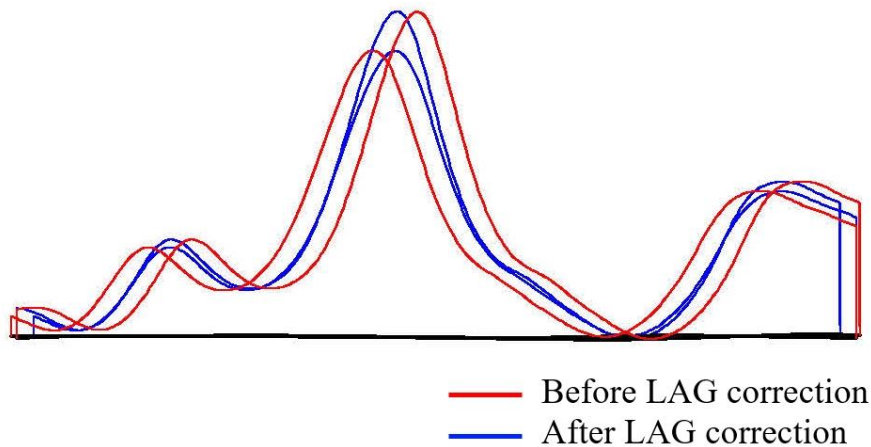


Figure 7: LAG test result.

4.2.3 Magnetic Heading Effect

The magnetic heading effect was determined by flying a cloverleaf pattern oriented in the same direction as the survey lines and tie lines. At least one pass in each direction was flown over a recognizable magnetically "flat" feature on the ground to obtain sufficient statistical information to estimate the heading error. This test results are shown as follows (Table 10, Figure 8).

Table 10: Results of the flown heading test..

Line	Direction	Mag (nT)	Height (m)
L0	0°	56522.0	3065
L90	90°	56522.3	3065
L180	180°	56520.5	3065
L270	270°	56522.3	3065
		56521.8	

/Geosoft Heading Correction Table

/		
/=	Direction:real:i	
/=	Correction:real	
/		
/	Direction	Correction
	0	-0.2075
	90	-0.4975
	180	1.2625
	270	-0.5575

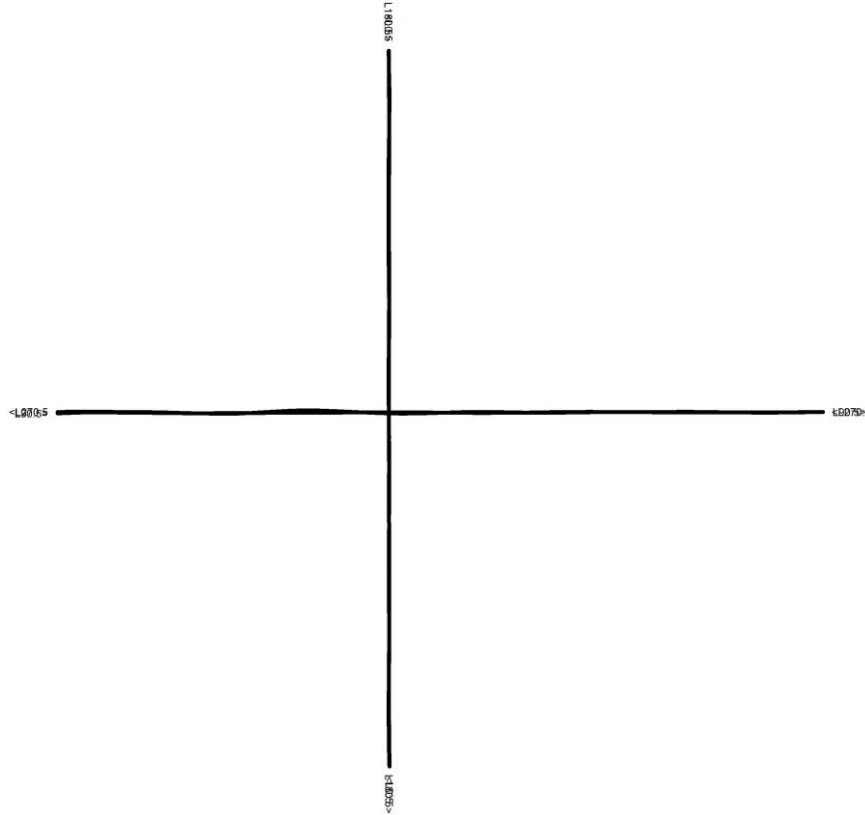


Figure 8: Cloverleaf flown during the Heading test.

4.2.4 Altimeter test – Radar/Barometric/DGPS

The altimeter calibration test was carried out by flying at the nominal heights of 80, 100, 150, 200, 250 and 300 m. This test is relevant because the elevation can directly interfere with concentration count in certain situations. In addition, barometric equipment may change with pressure and temperature.

The results of this test are displayed as follows in Figure 9 and Table 11.

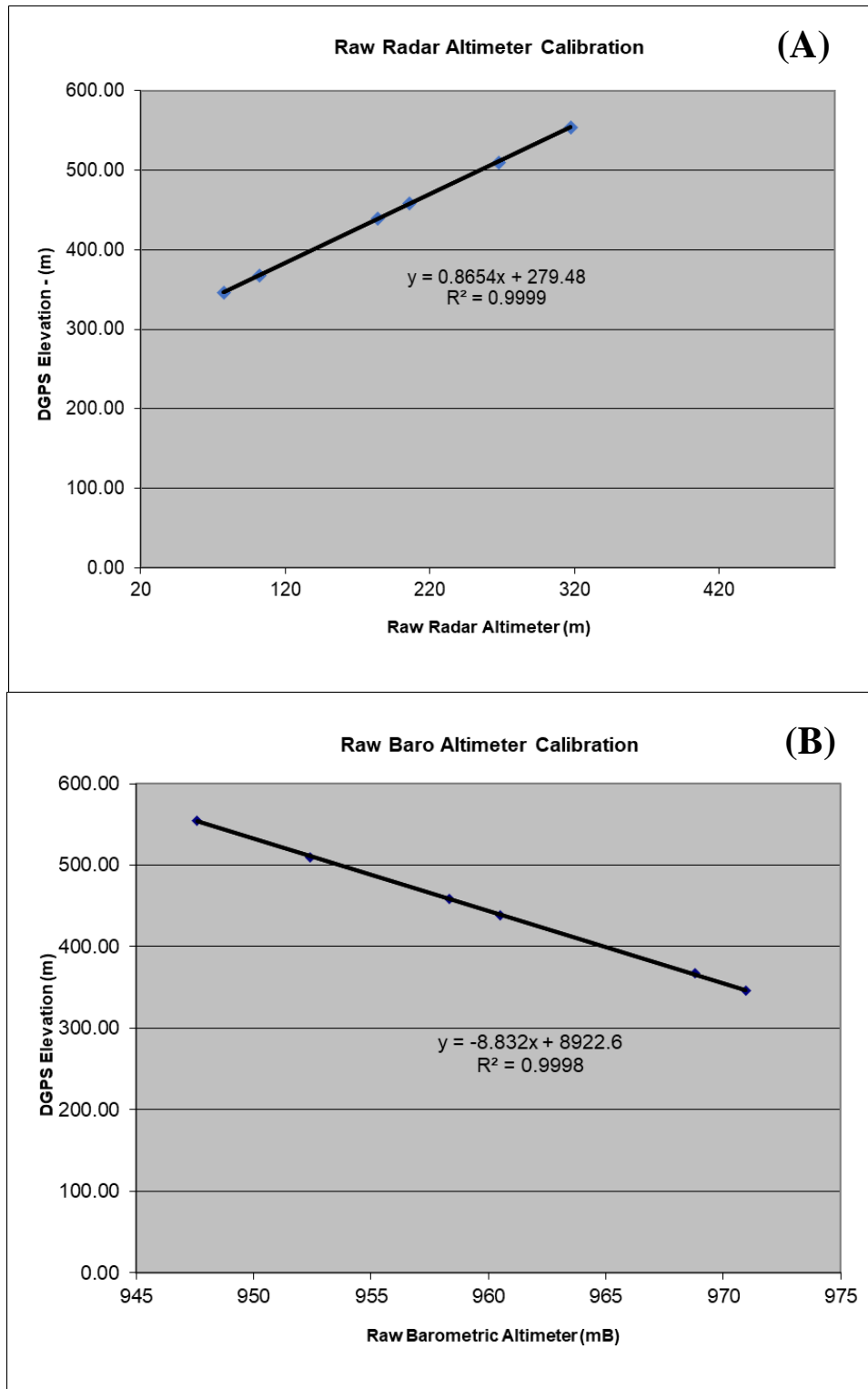


Figure 9: Results of the Radar/Barometric/DGPS altimeter test. Correlation coefficient in (A) = 0.9999; correlation coefficient in (B) = 0.9999.

Table 11: Altimeter test measured values.

Nominal Alt (m)	Raw Baro Elev. (mB)	Raw GPS Elev. (m)	Raw Radar (m)	Calibrated Radar (m)	Calibrated Baro (m)
80	970.95	346.20	77.60	346.64	347.20
100	968.80	367.80	102.00	367.75	366.19
150	960.50	439.02	184.00	438.72	439.49
200	958.35	458.50	205.80	457.58	458.48
250	952.40	510.00	267.50	510.98	511.03
300	947.60	554.30	317.40	554.16	553.43

DGPS-Raw Radar Slope =	0.865396	DGPS-RAW Radar Int =	279.482
DGPS-Raw Baro Slope =	-8.832013	DGPS-RAW Baro Int =	8922.642

4.3 VLF Checks

VLF checking procedures are based mainly upon transmitter functionality and operational procedures during the installation of the system into the aircraft of minor relevance for these purposes. Main factors are here described as follows.

4.3.1 VLF System Coupling

VLF system is composed of three (3) directional antennae components designated as LINE, ORTHO, and ERECT. LINE couples maximally with a field in the nominal direction of flight, ORTHO couples with a field at 90° to the direction of flight, and ERECT couples with the vertical field. The field parameters which are computed by the system are determined relative to the principal axis signal, which may be designated as either Line or Ortho.

On the other hand, traverse lines are disposed such as they go as perpendicular as possible to the main geological features orientation, hence the desirable field to measure by the VLF system is the one that propagates in the closest direction to the traverse lines. The transmitter stations that produce such signal are those located as perpendicular to the traverse line’s orientation as possible (based on electromagnetic theory), being the signal received named as LINE data.

In addition, the radiated field may be composite of any of three waves propagating from the transmitting antenna: the surface wave, the direct wave, and the sky wave. The combination of the first two waves is called “ground wave”. The sky wave reaches the receiver by reflection from ionized layers above the Earth. The ground wave provides most of the signal energy received at distances 100 to 300 km, and as distance increase, effects of the sky wave component cause cyclic variations in the intensity of the composite field. The magnitude of the ground wave field component is inversely proportional to the distance.

From above mentioned considerations, transmitter stations must be selected among those that have the power enough to reach the receiver with sufficient energy, not too far away to avoid increasing sky reflected interference signal and receive a proper ground wave energy, and considering coupling with the line direction.

The transmitters that meet such conditions are those located in northern USA, as follows:

- *NAA Cutler, Maine, USA* (44°39'N; 67°17'W), 24 kHz operating frequency, 1000 kW power. Approximately at 1,988 km away from survey site.
- *NLM LaMoure, North Dakota, USA* (46.3659°N; 98.3356°W), 25.2 kHz operating frequency, 500 kW power. Approximately at 572 km away from survey site.

The coupling with the NAA transmitter resulted in an angular difference of **16.76°** relative to the traverse line orientation (N-S/0°). The NLM resulted in angular difference of **42.52°**. Therefore, NAA transmitter was selected as the LINE signal, and the NLM transmitter as the ORTHO signal. Only traverse lines were used for processing and delivering final database because of the coupling. **Careful use of the ORTHO data is advised since the coupling angle is not ideal (out of the 60-90° recommended range).**

4.3.2 Schedules of the Transmitter Stations

VLF radio transmitter stations are placed around the world, and each one of them have programmed weekly maintenance and operation schedules. NAA station is not available from 10:00 to 18:00 UTC each Monday due to maintenance and from 18:00 to 20:00 UTC because of operator training. NLM station programmed maintenance on Tuesdays, from 12:00 to 19:00 UTC.

5.0 Quality Control and Data Processing

Daily quality control check of GPS positions and archiving of the data were completed by MPX at the Toronto, Ontario office using Geosoft's Oasis Montaj software.

All data were verified upon receipt, and checked against the flight logs. The final data processing, map and report preparation was completed by MPX at the Toronto, Ontario office.

5.1 *In-Field Processing and Deliverables*

The following items were verified once the data arrived in the Toronto, Ontario office for final processing and grid preparation.

5.1.1 Flight Path Compilation

The flight path was derived from differentially corrected GPS positions from the airborne data. A position was calculated ten times each second (approximately every 8 m along the flight path). The position data were then merged into the magnetic and radiometric data in each of the respective Geosoft GDB databases.

5.1.2 Digital Terrain Model

A digital terrain model (DTM) channel was calculated by subtracting the filtered radar altimeter data from the GPS elevation defined by the WGS84 ellipsoidal height.

The DTM channel was gridded using a minimum curvature algorithm with a grid cell size of 1/5 lines spacing and inspected for continuity. Micro-levelling of the DTM was then completed prior to DTM grid production.

5.1.3 Base Station Magnetic Data

The base station magnetometer data was edited, plotted and merged into the database on a daily basis. The following constraints were used during the quality control procedure:

- Removal of spikes in the data set resulting from cultural activities not associated with the survey (e.g., a truck driving by the base station);
- Diurnal Total Magnetic Intensity linear gradient could not exceed 12 nT in a straight-line chord over 5 minutes.
- Calculation of the 4th difference noise of the signal to identify potential erroneous data

5.2 *Airborne Magnetic Data*

Field processed magnetic data were made available on a daily basis and at the completion of the survey prior to demobilization of the survey aircraft and crew. A description of all processing methods applied to the magnetic data is included below.

5.2.1 Corrections

The processing of the data involved editing raw magnetic data to remove any noise spikes, maneuvers compensation was real-time performed by the DAARC system using the fluxgate magnetometer records, correcting for diurnal variations by using the digitally collected ground base station magnetic values, compensating the heading and LAG effects, and network adjustment using the traverse-line and control-line information to level the survey data set. The corrected data set was used to generate the initial Total Magnetic Intensity (TMI) grid upon which all further processing and analysis has been made.

The diurnal correction was applied using the averaged magnitude datum as follows (Table 12):

Table 12: Base-station magnetic datum.

Block	Base-mag Datum
Dryden Block	56,187.0 nT

5.2.1.1 Micro-levelling

After applying the above corrections to the magnetic profile data, residual line-direction-related noise was removed through the application of microlevelling. The microlevelling technique involves directional and high pass filters to produce a grid containing noise only in the line direction. In order to differentiate between noise and signal, the grid is extracted to the profile database, and an amplitude limit and a filter length are determined such that the final error channel reflects only noise present in the grid without removing or changing the geologic signal. This error channel is then subtracted from the initial data channel to obtain the final microlevelled channel. That microlevelled channel is then gridded using a minimum curvature algorithm. Finally, the resulting grid is, therefore, free of line direction noise.

5.2.2 Gridding

The corrected magnetic line data was interpolated between survey lines using a random point minimum curvature gridding algorithm to yield x-y grid values for a standard grid cell size of 1/5th of the traverse line separation (15 m cell size).

5.2.3 Filter Derivatives

The Total Magnetic Intensity (TMI) data were subjected to:

- Subtraction of the International Geomagnetic Reference Field (IGRF)
- Calculation of the First Vertical Derivative (1VD)
- Calculation of the Analytic Signal Grid (AS)
- Calculation of the Horizontal Derivative (HDR)
- Calculation of the TMI reduced to the Earth's magnetic pole (RTP)

Colour grids were produced for all the above listed magnetic products. The mentioned spatial filtering techniques were completed using the Oasis Montaj MAGMAP and IGRF modules for filtering in the 2D FFT domain.

5.2.3.1 IGRF Removal (TMI-IGRF)

The International Geomagnetic Reference Field (IGRF) is a long-wavelength regional magnetic field calculated from permanent magnetic observatory data collected worldwide. The IGRF is updated and determined by an international committee of geophysicists every five (5) years. Secular variations in the Earth's magnetic field are incorporated into the determination of the IGRF. The IGRF values were calculated from the new-released model of the year 2020 and using the parameters described in Table 13.

Table 13: IGRF calculation parameters.

Block	IGRF Information				
	Date	Altitude	Inclination	Declination	IGRF (mean)
Dryden Block	2021/11/06	475 m	74.57°	-1.00°	56,537.5 nT

By removing the IGRF from the observed Total Magnetic Intensity (TMI), the resulting residual magnetic intensity allows for more valid modelling of individual near-surface anomalies. Additionally, the data can be more easily incorporated into databases of magnetic data acquired in the past or surveyed in the future.

5.2.3.2 Calculation of the First Vertical Derivative (1VD)

To "sharpen" magnetic anomalies and to provide a better spatial location of source axes and boundaries, a first vertical derivative map was computed from the TMI. Vertical derivatives calculate the rate of change of the TMI as it drops off when measured vertically over the same point (upward continuation). Potential field data obeys Laplace's equation, which allows for the computation to take advantage of this symmetry and solve the vertical or "z" component of the field.

5.2.3.3 Analytic Signal

This tool presents magnetic anomaly information stripped of the dependence on the inclination of the Earth's inducing field, so these anomalies are positive and sit directly over their sources. It is a suitable technique to locate magnetized bodies and geological contacts.

5.2.3.4 Reduction-to-the-Magnetic-Pole (RTP)

To compensate for the shift of the true anomaly position over the causative source, due to the magnetic inclination and declination, the magnetic data was recomputed so that magnetic anomalies will appear as they would if located at the north magnetic pole. The result of this operation is that in theory, the magnetic anomaly is located directly over top of the causative source. The computation is referred to as "reduction-to-the-pole" (RTP). The reduction-to-the-pole is computed using a FFT (Fast Fourier Transform) operator.

The RTP not only shifts the anomalies to their correct position with respect to the causative magnetic bodies but assists in the direct correlation and comparison of magnetic anomalies, trends, structural axis, and discontinuities with mapped geologic surface expression.

The RTP was computed using the following parameters for the survey area (Table 14):

Table 14: RTP calculation parameters.

Block	RTP Parameters	
	Inclination	Declination
Dryden Block	74.57°	-1.00°

5.2.3.5 Calculation of the Horizontal Derivative (HRD)

Calculated from horizontal X and Y directional derivatives enhances the magnetic gradients on the horizontal plain of observation.

5.3 Airborne Radiometric Data

5.3.1 Background for Corrections and Processing

Gamma-ray spectrometer surveys are utilized for mapping the concentration and distribution of naturally occurring radioelements. The use of an airborne gamma-ray spectrometer allows for the in-situ analysis of

radioelement concentrations of naturally occurring Potassium (K), Uranium (U) and Thorium (Th) in the field.

To the geologist, maps of the concentrations of K, U, and Th can prove diagnostic in the mapping of rocks and soils as an aid in geologic mapping and in the exploration for uranium, gold, tin and tungsten deposits where the primary mineralization process is often related to K metasomatism.

Radioactivity measurements from an airborne platform are dependent upon the detection of gamma rays produced through the radioactive decay of the nuclide to be detected. Only three radioactive elements emit sufficient gamma radiation to be measured by airborne methods. The three major sources are:

- Potassium-40 (40K) which comprises 0.011% of all potassium
- Daughter products from the ^{238}U decay series,
- Daughter products from the ^{232}Th decay series.

Spectrometers require a finite time to process each pulse from the detector. While one pulse is being processed, all other incoming pulses are automatically rejected. The total counting time available is thus reduced by the time taken to process all pulses (the "dead time"). The time during which the spectrometer is receptive to incoming pulses is the "live time". The dead time is therefore the difference between the sample accumulation time and the live time, and must be compensated.

Airborne gamma-ray spectrometer surveys can detect high energy cosmic rays of non-terrestrial. This cosmic radiation interacts with molecules in the atmosphere, the aircraft, and the NaI detectors resulting in the production of high energy radiation. This radiation is detectable and increases exponentially with height above sea level and must be compensated for to obtain reliable and repeatable measurements and detection of terrestrial radiation sources.

The traditional energy windows used to detect gamma-ray radiation from K, Th, and U sources have overlapping areas where the energy recorded for a given element contains some contribution from all three radioelements. A correction procedure, known as stripping, is applied to the data to compensate for this spectral overlapping.

The natural gamma-ray spectrum over the range of 0 to approximately 3000 keV (Figure 10) is resolved by the spectrometer used into 1024 channels, each channel having a width of ~2.93 KeV. A separate channel records all high energy radiation above 3000 KeV, the cosmic radiation contribution. Within the defined radioelement windows, the counts recorded are summed over a given time period.

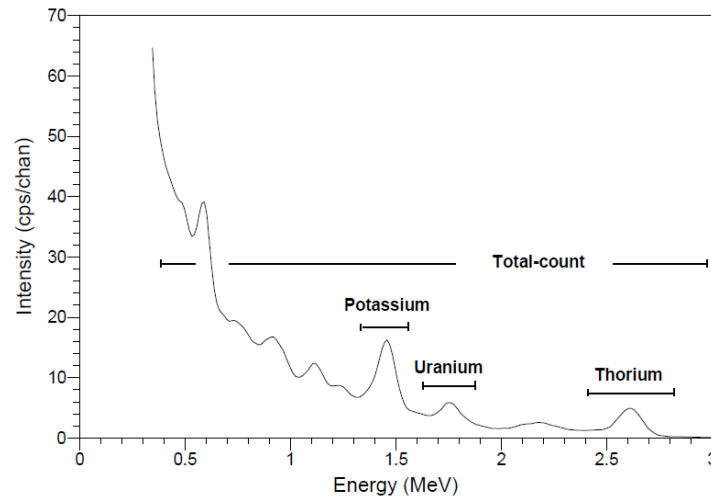


Figure 10: Typical airborne gamma-ray spectrum showing the positions of the conventional energy windows.

Care must be taken during the acquisition of gamma-ray spectrometer data as the contribution from radon gas and related decay products in the atmosphere can result in misleading count rates. Radon gas can also diffuse from the ground, but only one radon nuclide is directly related to the Uranium decay series. In order to minimize the impact of radon "contamination," radiometric surveys are not completed during rain (since it "washes" radon from the air and increases ground concentrations) or fog conditions and for a period of not less than 2 hours after precipitation has finished in order to allow for dispersion of radon gas to normal background levels.

In airborne surveying the height of the detector changes continuously as the aircraft proceeds along the lines, and the window data must be corrected to a nominal survey height since count rates vary approximately exponentially with height.

Radiometric surveys have limited depth penetration; most radioactive sources being within the upper 1.5 m of the ground. Radiometric surveys are therefore not effective over water bodies or snow-covered areas, the presence of water (in either liquid or solid state) effectively masking radiometric sources.

5.3.2 Processing Applied Using the Geosoft Oasis Montaj Radiometric Processing System

The reduction of radiometric data followed standard processing steps as outlined in the recommendations of IAEA-TECDOC-1363 - Guidelines for radioelement mapping using gamma-ray spectrometry data.

The corrections to the radiometric data involved:

1. Correction for system dead-time,
2. Background removal,
3. Cosmic correction (Compton scattering correction)
4. Stripping ratios
5. Attenuation Correction (corrected to the nominal height AGL per block)
6. Conversion of count rates to ppm values
7. Calculation of radioelement's ratios (Th/K, U/K and U/Th ratios)

Following the above standard corrections, the Geosoft Oasis Montaj Radiometric Processing System (RPS) software package was used to process the radiometric data finally. The data was processed using

the standard window (ROI) technique, which follows the IAEA standards and is the simplest method for processing natural radiation data. The standard window (ROI) technique was thought to provide the most geological information and is the method used in the data presented.

As part of the processing step, the digital elevation model (DTM) is calculated by subtracting the laser altimeter from the GPS elevation. The laser altimeter is calibrated using the GPS altimeter. The DTM is calculated to provide information on the topography for the interpretation of the radiometric data.

5.3.2.1 Reduction to elemental concentrations

It consists of the conversion of count rates into ground concentrations of the radioelements. The procedure is performed by dividing each corrected window count rate by a "sensitivity" coefficient. The coefficient for each window is estimated from data acquired from airborne flights over a calibration range. The derived results comprise the equivalent concentration of Thorium (equiv Th-ppm), Uranium (equiv U -ppm) and percentage of Potassium (%K).

5.3.2.2 Total Air Absorbed Dose Rate

The total counts measured during this survey were converted into an equivalent radiometric natural air absorbed dose rate in nanoGrays per hour (nGy/h) using a calibration factor of 23 cps/nGy/h that was applied to background corrected and stripped total count values.

Formulae are presented below to demonstrate the relationship between two units commonly used to show total radiometric counts; *nanoGrays per hour (nGy/h)* and *microRöntgens per hour (μR/h)*.

The natural air absorbed dose rate used in this report can also be calculated from the potassium (%K), equivalent uranium (ppm), and equivalent thorium (ppm) concentrations (GSC, 2006):

$$\text{Natural Air Absorbed Dose Rate (nGy/h)} = 13.08 \text{ K} + 5.43 \text{ eqU} + 2.69 \text{ eqTh}$$

Traditionally radiometric total count values have been converted into natural exposure rates and reported as micro Röntgens per hour (μR/h). The formula for this calculation is provided below for convenience but was not used in this report (Grasty et al., 1984).

$$\text{Natural Exposure (μR/h)} = 1.505 \text{ K} + 0.625 \text{ eqU} + 0.31 \text{ eqTh}$$

5.3.2.3 Radioelement's ratios (Th/K, U/K & U/Th)

The radioelement's ratios are calculated by statistical normalized radioelements K, U and Th (Minty, 2011). Ratios consist on arithmetic combinations of radioelement grids and the effect of environmental factors on radiometric response are less evident on them. Therefore, they often correlate more highly with geological units. Also, ratios are useful during interpretation because subtle features are often shown that are not apparent on the original grids.

5.3.2.4 Ternary map

The Ternary Map consists of a colour composite image generated by modulating the red, green and blue (RGB) phosphors of the display device in proportion to K, Th, U and TC grids' radioelement concentration values. The use of the RGB scale for K, Th and U, respectively, is standard for displaying gamma-ray data. A similar normalization technique for ternary imaging can also be followed using the CMY scale standard (cyan, magenta, yellow). In addition, sum-normalization is applied to reduce the

effects of the attenuation of gamma-rays by environmental factors. Provided the sum-normalized channels are linearly stretched, the chromatic colour variations are proportional to the relative radioelement abundance of K, U and Th over the survey area. The channels can be quantitatively related to the ternary legend.

Although ternary images may display either very dark or light colours (close to black and white respectively), ternary images do not include any shading/shadowing effect. These dark/light colours come from the composition of the three bands (RGB close to either 0-0-0 or 255-255-255 respectively) in areas of either much or little abundance of the three normalized element concentrations (U, Th and K).

5.4 Airborne VLF data

5.4.1 Polarity Compensation

The polarity sign of the quadrature data is stored by the system, indicating the in- and out-of-phase vertical component relative to the magnetic field. Therefore, to match the anomalies and compensate this difference, such signs must be changed according to the heading on which each line was flown. For this project, all line data recorded facing northwards were sign inverted multiplying data by -1, and line data recorded facing southwards were not changed. Nevertheless, this convention can be easily changed by multiplying the entire final quadrature channel data by -1, if the ultimate user/interpreter requires and/or wants the anomalies displayed as the other option.

5.4.2 Correction of Time Variations

As survey area is far away from transmitter station, reflected sky waves interfere in the total field records in cyclic variations. Thus, shift compensations are required for leveling data recorded during different flights and times during the day, and among days. When single flights are long enough to record these cycles, and as they increase while distance to transmitter increases, sometimes shift compensations were required on data acquired during a same flight. This is made comparing some anomaly magnitudes between contiguous flights and averaging the difference between both by a constant value. It aims to make the anomalies continuous to represent readable geological features.

5.4.3 Parallax Correction (LAG)

Since survey lines were flown alternately in opposite directions, the electronic delays during recording resulted in values being shifted systematically. In order to compensate the so-called "herringbone" effect, a 2 seconds LAG correction was applied on VLF data.

5.4.4 Micro-leveling

As the information from control lines is useless in VLF data for leveling purposes (because of the rotation of the antennae), any residual level difference must be solved by applying a combination of Butterworth and Directional Cosine filters for extracting de-corrugation noise from data. Then this noise was evaluated and removed from data. Process step applied to both total field and quadrature.

5.4.5 Conversion into percentage values

Output data unit is Volt, relative to the 100% primary field magnitude from the calibration of the system during ground tests and measured during survey as zero (by offsetting this magnitude down to zero, the system can record anomalies of >100% primary field magnitude). The ceiling of the system's sensitivity for this survey is 10 V; it represents the 100% magnitude of change that the system may record. Therefore, multiplying both total field and quadrature by 10, data were converted into percentage.

Note: the occurrence of high-transmission power lines across the area would introduce artifacts into data.

6.0 Deliverable Products

The survey data are presented as Geosoft digital databases (*.GDB). Gridded data are delivered as Geosoft grids (*.GRD). Map files are provided as GeoTIFF (*.tif) and packed Geosoft Map formats.

Three (3) separate databases were delivered per survey block and data type (magnetic, radiometric, and VLF).

In addition, the maps were prepared at the following scale:

- 1:20,000 for Dryden Block related products.

According to the above-illustrated scale, the following maps were produced in GeoTIFF and Geosoft Packed formats:

Magnetic Maps (colour image at 300 dpi, grid names are in parenthesis):

- Flown flight path
- Total magnetic intensity (TMI)
- Total magnetic intensity after IGRF removal (TMI-IGRF)
- Calculated first vertical derivative (1VD)
- Analytic signal of the total magnetic intensity (AS)
- Calculated horizontal derivative (HDR)
- Total magnetic intensity reduced to the Earth's magnetic pole (RTP)
- Computed Digital Terrain Model (DTM)

Gamma-Ray Spectrometry Maps (colour image at 300 dpi, grid names are in parenthesis):

- Total air absorbed dose rate (TC)
- Percentage of Potassium (K)
- Equivalent Concentration of Thorium (Th)
- Equivalent Concentration of Uranium (U)
- U/Th normalized Ratio (ratio_UTh)
- U/K normalized Ratio (ratio UK)
- Th/K normalized Ratio (ratio ThK)
- Ternary Map (ternary)

VLF Maps (colour image at 300 dpi, grid names are in parenthesis):

- Line Total Field - Hy (TOT_LINE)
- Line Quadrature - Hz (QUAD_LINE)
- Ortho Total Field - Hy (TOT_ORTHO)
- Ortho Quadrature - Hz (QUAD_ORTHO)

All map products were projected on WGS84, UTM Zone 15N, with Latitude/Longitude edge ticks.

6.1 Digital Data

The edited field and processed digital data were delivered to the Client.

The grids were prepared in WGS84, UTM Zone 16N datum and projection method, as Geosoft Grid format as listed in the previous section hereabove. The grids were interpolated at a cell size of 1/5 of the

line spacing (15 m).

6.1.1 Metadata Files

Text files with information about the digital data provided for survey block (metadata) are made available for the survey. All files and/or database channels are described in the metadata file.

See Appendix 2 for the contents of the metadata file.

6.2 Report

This report provides information about the acquisition, processing and presentation of the survey data.

6.2.1 Statement of Qualifications

The collection of data and preparation of map and report products for this project were completed by the following staff of MPX: Daniel McKinnon, Stephen Williams, Tonia Bojkova, Marco Nieto, Fabian Linares and Jesus Piña. A summary of their qualifications appears in Appendix 1.

Respectfully submitted,

MPX Geophysics Ltd.

Appendices

Appendix 1. Statement of Qualifications	32
Appendix 2. Digital File Metadata	34
Appendix 3. Project Status Report.....	38

Appendix 1. Statement of Qualifications

Daniel J. McKinnon, President

Daniel started his career in the base metal mines of New Brunswick (Canada). He has worked extensively in North and South America, Asia and Europe.

He has been associated with MPX since 2006 and, through a hands-on approach to operations, has developed a comprehensive understanding of the business, with key elements of his personality, namely attention to detail, safety and teamwork, becoming indelibly imprinted on the corporate ethos of the organization. He sets high standards in all aspects of MPX's operations, from detailed safety procedures to the quality of the equipment used.

Aided by his handpicked team of professionals, coupled with astute leadership and personal commitment, he has been privileged to see the company expand, succeed and prosper.

Under his steadfast direction, MPX has been propelled to higher levels of service based on the fundamental strategies of Industry-leading safety practices, value to the customer, commitment to socialization programs in the countries in which our projects are conducted and the prioritization of the involvement/interaction with the local communities

Stephen Williams, Project Manager, B.Sc, Senior Geophysicist

Stephen has more than 40 years of experience as a geophysicist and over 30 years in airborne. He has a B.Sc. in Geophysics and is a former GM of Geotech Middle East, VP at Aeroquest, Operations Manager at World Geoscience and VP Airborne Gravity Fugro-LCT. Stephen has extensive international and domestic operational and managerial skills, actively participating in surveys in over 40 countries and all seven continents. His knowledge and experience extend to petroleum and mineral exploration – Stephen has case studies published in Offshore and Oil & Gas magazines utilizing potential fields programs and specific gravity data.

Tonia Bojkova, M. Sc., Senior Geophysicist

Tonia received her first Master of Science degree in Engineering Geophysics at the University of Mining and Geology in Sofia, Bulgaria, where her thesis research focused on integrating and interpreting high resolution magnetic and radiometric data collected over southeastern Bulgaria. The best method to determine regional magnetic models without the influence of local anomalies was investigated during her second Master of Science degree obtained in Applied Mathematics at the Technical University in Sofia, Bulgaria. Tonia entered the industry in 1980 as a geophysicist for the Bulgarian government, collecting, processing, and analyzing airborne radiometric and magnetic data while also performing gamma-ray monitoring of Bulgaria after the Chernobyl NPP fallout.

Tonia has 40 years of continuous experience in the geophysical survey industry with extensive experience processing and interpreting airborne magnetic, radiometric, and electromagnetic (EM) data.

Tonia has been an integral component of the MPX team since its incorporation in 2006.

Gordon Roberts, Geophysicist, B.Sc Geology, Business Development Manager

Gord is an experienced Professional Geoscientist with over 30 year's in Airborne Geophysics. His experience and knowledge is in all aspects of the Mining, Non-Mining and O&G industry, including all Airborne Technologies, Data Processing and Interpretation, Executive Management, Financial Markets and Business Development. This experience over the years has been in various roles with Geotrex, Geotrex-Dighem, CGG, Fugro Airborne Surveys and CGG Multi-Physics. He has International experience with overseas postings in Paris, Australia, Argentina and Cairo, as well as business visits to 75 countries globally.

Marco Nieto, M. Sc., Senior Geophysicist, PGeo.

Marco obtained his Geologist degree at Universidad Nacional de Colombia and studied a Master in Science in Geophysics at the University of Western Ontario in London, Ontario. His 15 years of experience in Geophysical and Geological Exploration are focused on metal ore deposit exploration. He has used potential methods for Mining, Oil and underground water exploration in different countries of the Americas.

Besides, Marco is a Practicing Member of the Association of Professional Geoscientists of Ontario and a fellowship of the Society of Economic Geologists. He also has a Master in Business Administration at the University International of La Rioja (Spain).

Marco has supported the MPX team since 2014.

Fabian Linares, B.Sc., Senior Geophysicist

Fabian is a Geophysical Engineer who graduated at the Central University of Venezuela in 2013, and he is a current candidate for M.Sc. in Geology. He has more than six years of experience in both Oil & Gas and mineral exploration. He has worked in 3D seismic, electrical sounding, and ground/airborne potential-method surveys and interpretations (magnetic, gravity, radiometric, EM and VLF data), including also satellite-combined gravity and magnetic models. During the last three years, Fabian has served as Geophysicist at MPX Geophysics in survey operations as field QA/QC and processing and interpretation projects worldwide.

Jesus Piña, Senior Field Operator

He is a Computer Systems engineer who graduated from the University of Guadalajara in 2006 and mechatronic technician from the Technological University of Chihuahua in 2011.

Jesus has more than ten (10) years of experience in geophysical exploration and six (6) more in aviation-related matters. During this time, Jesus has been in charge of the administration and control of maintenance and spare parts of a helicopter company, where he was also responsible for having applied methods of control and training of personnel. In the last ten years, he has served as Project Manager and Field Operator at MPX Geophysics, leading projects successfully in 8 different countries throughout the Americas.

Appendix 2. Digital File Metadata

Table 15: File names and descriptions for all digital data prepared.

Dryden, Airborne Magnetic/Radiometric/VLF Survey.

Grids: WGS84 Datum, UTM Zone 15N Projection

P21084_TMI.grd	Leveled Total Magnetic Intensity – nT (TMI)
P21084_TMI_IGRF.grd	Leveled TMI, IGRF removed – nT (TMI-IGRF)
P21084_1VD.grd	Calculated first vertical derivative – nT/m (1VD)
P21084_HRD.grd	Calculated horizontal derivative – nT/m (HRD)
P21084_RTP.grd	TMI reduced to the magnetic pole – nT (RTP)
P21084_AS.grd	Analytic signal of the residual magnetic intensity – nT/m
P21084_TC.grd	Total Air Absorbed Dose Rate - nGy/h
P21084_K.grd	Equivalent concentration of Potassium - %K
P21084_Th.grd	Equivalent concentration of Thorium - eqTh ppm
P21084_U.grd	Equivalent concentration of Uranium - eqU ppm
P21084_UTh_Ratio.grd	U/Th Ratio
P21084_ThK_Ratio.grd	Th/K Ratio
P21084_UK_Ratio.grd	U/K Ratio
P21084_DTM.grd	Calculated Digital Terrain Model – m (DTM)
P21084_TOT_LINE.grd	VLF Line Total Field (Hy) - % (TOT_LINE)
P21084_QUAD_LINE.grd	VLF Line Quadrature (Hz) - % (QUAD_LINE)
P21084_TOT_ORTHO.grd	VLF Ortho Total Field (Hy) - % (TOT_ORTHO)
P21084_QUAD_ORTHO.grd	VLF Ortho Quadrature (Hz) - % (QUAD_ORTHO)

Maps: WGS84 Datum, UTM Zone 15N Projection

***Note that a GeoTIFF image and a Geosoft Packed map have been created for each grid above listed. The file name structure is the same as the grid files with .tif or .map extension instead of the ".grd."**

Only two additional maps were provided (not included into the list of grids) for the following:

P21084_Ternary	Ternary image - %K-eqU-eqTh – RGB
P21084_FlightPath	Flown flight path map

Magnetic database: P21084_MAG.gdb

Channel Name and description:

X_WGS84_15N	Easting – WGS84 UTM 15N (metres)
Y_WGS84_15N	Northing – WGS84 UTM 15N (metres)
Longitude	Longitude (Geographic WGS84) (degrees)
Latitude	Latitude (Geographic WGS84) (degrees)
GPSalt	GPS height (meters)
Date	Flight date (YYYYMMDD)

Flight	Flight number
FIDN	Fiducial number
Diurnal	Earth's magnetic field diurnal variation (nT)
Line	Line number channel
UTCtm_sec	UTC time (start of day) (seconds)
Radar_m	Radar Altimeter (meters)
DTM	Calculated Digital Terrain Model (meters)
Mag_BS	Magnetic Base Station (nT)
VMX	Magnetic fluxgate data in direction X
VMY	Magnetic fluxgate data in direction Y
VMZ	Magnetic fluxgate data in direction Z
TMI	Final levelled and micro levelled Total Magnetic Intensity (nT)
IGRF	International Geomagnetic Reference Field (nT)
Incl	IGRF Inclination (degrees)
Decl	IGRF Declination (degrees)
UncMag1	Uncompensated raw magnetic data (nT)
CmpMag1	Compensated raw magnetic data (nT)
Mag_CD	Diurnal corrected CmpMag (nT)
Mag_CDHL	Diurnal, Heading and Lag corrected CmpMag (nT)
TMI_IGRF	Final Total Magnetic Intensity, IGRF removed (nT)

Radiometric database: P21084_SPEC.gdb

Channel Name and description:

X_WGS84_15N	Easting – WGS84 UTM 15N (metres)
Y_WGS84_15N	Northing – WGS84 UTM 15N (metres)
Longitude	Longitude (Geographic WGS84) (degrees)
Latitude	Latitude (Geographic WGS84) (degrees)
Date	Flight date (YYYYMMDD)
Flight	Flight number
FIDN	Fiducial number
UTCtm_sec	UTC time (start of day) (seconds)
GPSalt	GPS height (meters)
Line	Line number channel
rDwn	Number of Down-looking crystals
rDataD	Full spectra from Down-looking crystals
rUp	Number of Up-looking crystals
rLiveT	Live Time for Down-looking crystals (ms)
rDataU	Full spectra from Up-looking crystals
Radar_m	Radar Altimeter (meters)
Temp	Temperature in C°
Baro_mB	Barometric (mB)
RALTSTP	Radar Altitude corrected for TSTP (m)

TC_raw_D	Raw Total Count channel from Down looking crystals (cps)
K_raw_D	Raw Potassium channel for Down looking crystals (cps)
Th_raw_D	Raw Thorium channel from Down looking crystals (cps)
U_raw_D	Raw Uranium channel from Down looking crystals (cps)
U_raw_Up	Raw Uranium channel from Up looking crystals (cps)
Cosmic_raw_D	Raw Cosmic channel from Down looking crystals (cps)
TC_final	Calculated total count down looking channel by using K, U, Th final (nGy/h)
K_final	Corrected Potassium from Down looking crystals (%K)
Th_final	Corrected Thorium from Down looking crystals (eqTh ppm)
U_final	Corrected Uranium from Down looking crystals (eqU ppm)
UTHRATIO	U/Th Ratio (normalized)
THKRATIO	Th/K Ratio (normalized)
UKRATIO	U/K Ratio (normalized)
DTM	Calculated Digital Terrain Model (m)

VLF databases: P21084_VLF.gdb

Channel Name and description:

X_WGS84_15N	Easting – WGS84 UTM 15N (metres)
Y_WGS84_15N	Northing – WGS84 UTM 15N (metres)
Latitude	Latitude - WGS84 (degrees)
Longitude	Longitude - WGS84 (degrees)
Date	Flight date (YYYY/MM/DD)
FIDN	Fiducial
UTCtm_sec	UTC time (start of day) (seconds)
GPStime	GPS time (hh:mm:ss.ss)
Radar_m	Radar altimeter elevation from surface (meters)
Flight	Flight number
GPSalt	GPS elevation (meters)
LINE	Line number
GPSsat	Available GPS Satellites
TOT_LINE_Raw	Raw Line Total Field (Volts)
TOT_LINE_TVLAG	Line Total Field after Time-variation and LAG compensations (Volts)
TOT_LINE_Lev	Line Total Field after levelling (Volts)
TOT_LINE_Final	Final Line Total Field Hy (%)
QUAD_LINE_Raw	Raw Line Quadrature (Volts)
QUAD_LINE_Sign	Raw Line Quadrature after flipping Polarity (Volts)
QUAD_LINE_LagLev	Line Quadrature after LAG and levelling compensations (Volts)
QUAD_LINE_Final	Final Line Quadrature Hz (%)
TOT_ORTHO_Raw	Raw Ortho Total Field (Volts)
TOT_ORTHO_TVLAG	Ortho Total Field after Time-variation and LAG compensations (Volts)
TOT_ORTHO_Lev	Ortho Total Field after levelling (Volts)
TOT_ORTHO_Final	Final Ortho Total Field Hy (%)

QUAD_ORTHO_Raw	Raw Ortho Quadrature (Volts)
QUAD_ORTHO_Sign	Raw Ortho Quadrature after flipping Polarity (Volts)
QUAD_ORTHO_LagLev	Ortho Quadrature after LAG and levelling compensations (Volts)
QUAD_ORTHO_Final	Final Ortho Quadrature Hz (%)

Report: P21084_CriticalRes_Report_2021.pdf

Appendix 3. Project Status Report

Table 16: Project Status Report.

GENERAL		KMS		HOURS			COMMENTS																																																																																				
DAY	DOY	Type	FLT#	Crew	Flown Km	Acc. Kms	Mob	Test	Survey	Total	REMARKS - Temp, weather, Status (See STATS Page for Wx Codes)				WX																																																																												
<table border="1" style="width:100%; border-collapse: collapse;"> <tr> <td colspan="2">Total Aircraft Kilometers</td> <td colspan="4">Total Aircraft Hours</td> <td colspan="2">Ln Kilometers Contracted</td> <td colspan="2">828</td> <td colspan="2">Activity Type Key</td> <td colspan="2">4</td> <td colspan="2">Production</td> </tr> <tr> <td>Flown</td> <td>Accepted</td> <td>Remaining</td> <td>% Done</td> <td>Mobilization</td> <td>Test/Train</td> <td>Survey</td> <td>Total</td> <td>Planned total Ln Kilometers</td> <td>827.6</td> <td>1</td> <td>Mobilization</td> <td>5</td> <td colspan="3">Weather / Project Delays</td> </tr> <tr> <td>828.7</td> <td>828.7</td> <td>-1.1</td> <td>100%</td> <td></td> <td>1:18</td> <td></td> <td>7:42</td> <td>9:00</td> <td>107.6</td> <td>2</td> <td>Installation</td> <td>6</td> <td colspan="3">Pilot day off</td> </tr> <tr> <td colspan="8"></td> <td>Ln-Kilometres per Hour</td> <td>207.2</td> <td>3</td> <td>Equipment troubles</td> <td>7</td> <td colspan="3">Standby No-Charge</td> </tr> <tr> <td colspan="8"></td> <td>Ln/day</td> <td></td> <td colspan="6"></td> </tr> </table>												Total Aircraft Kilometers		Total Aircraft Hours				Ln Kilometers Contracted		828		Activity Type Key		4		Production		Flown	Accepted	Remaining	% Done	Mobilization	Test/Train	Survey	Total	Planned total Ln Kilometers	827.6	1	Mobilization	5	Weather / Project Delays			828.7	828.7	-1.1	100%		1:18		7:42	9:00	107.6	2	Installation	6	Pilot day off											Ln-Kilometres per Hour	207.2	3	Equipment troubles	7	Standby No-Charge											Ln/day							
Total Aircraft Kilometers		Total Aircraft Hours				Ln Kilometers Contracted		828		Activity Type Key		4		Production																																																																													
Flown	Accepted	Remaining	% Done	Mobilization	Test/Train	Survey	Total	Planned total Ln Kilometers	827.6	1	Mobilization	5	Weather / Project Delays																																																																														
828.7	828.7	-1.1	100%		1:18		7:42	9:00	107.6	2	Installation	6	Pilot day off																																																																														
								Ln-Kilometres per Hour	207.2	3	Equipment troubles	7	Standby No-Charge																																																																														
								Ln/day																																																																																			
<table border="1" style="width:100%; border-collapse: collapse;"> <tr> <td>Planned Km</td> <td>827.6</td> </tr> <tr> <td>Previous Total</td> <td></td> </tr> <tr> <td>Total Km flown</td> <td>828.7</td> </tr> <tr> <td>Remaining Km</td> <td>-1.1</td> </tr> <tr> <td>Previous Aircraft Hours</td> <td></td> </tr> <tr> <td>Total Aircraft Hours</td> <td>9:00</td> </tr> </table>												Planned Km	827.6	Previous Total		Total Km flown	828.7	Remaining Km	-1.1	Previous Aircraft Hours		Total Aircraft Hours	9:00																																																																				
Planned Km	827.6																																																																																										
Previous Total																																																																																											
Total Km flown	828.7																																																																																										
Remaining Km	-1.1																																																																																										
Previous Aircraft Hours																																																																																											
Total Aircraft Hours	9:00																																																																																										

Notes:

Personnel Key (Pers.)	1	Daniel McKinnon, MPX CEO
	2	Tonia Bojkova, Senior Geophysicist
	3	Marco Nieto, Business Development Director - Geophysicist
	4	Fabian Linares, Senior Geophysicist - Project Manager
	5	Jesus Pina, Equipment Technician
	6	Stephen Williams, Senior Geophysicist
	7	Pilot - Jay Matheson
	8	Pilot - Chris Bracker
	9	Pilot - Alex Smith
	10	
	11	
	12	
	13	
	14	
	15	
	16	
	17	
	18	
	19	
	20	
	21	

Equipment List:

Aircraft:	Piper Navajo PA31 Fixed Wing	Registration:	C-GQVP
Aircraft Velocity:		< =	150 Knots
Aircraft Altitude:	70m	Configuration:	Fixed Boom
Radar Altitude:	70m	Sampling:	20Hz
Magnetometer:	CS3	Sampling:	1Hz
Spectrometer:	Radiation Solutions RSX-5	Sampling:	20Hz
Radar Altimeter:	Bendix King	Sampling:	1 Hz
Aircraft GPS:	Novatel L1L2		
VLF system:	Totem 2A		
Base Mag (s):	GSM19		
Datum:	Beasemag A =		

Area #	KM	Name
1	827.6	Dryden Project

APPENDIX B:

Plan Map with Mavis Lake Claim Cells and Flight Path Boundary

Mavis Lake Lithium Project



WGS 1984 UTM Zone 15N

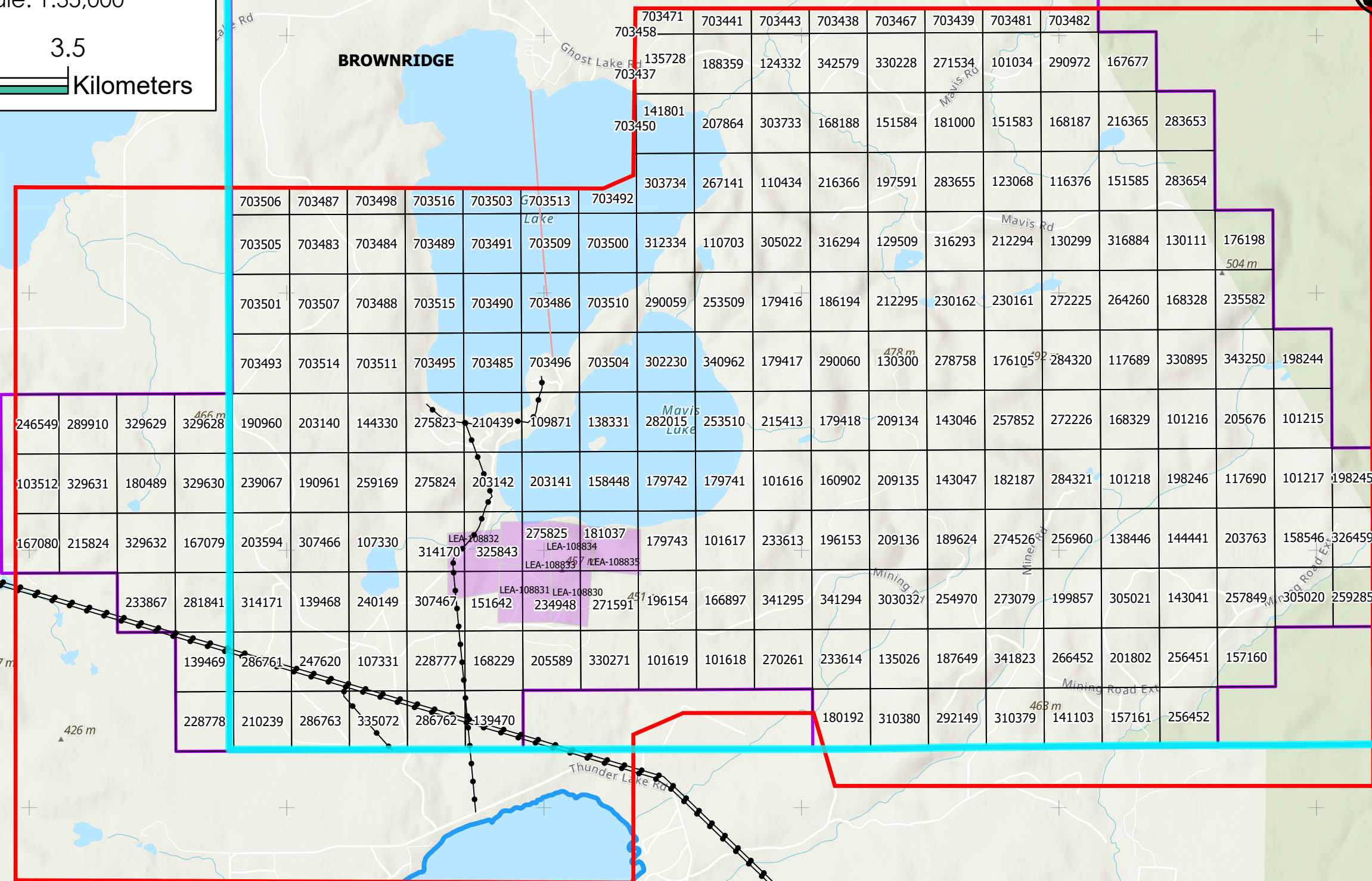
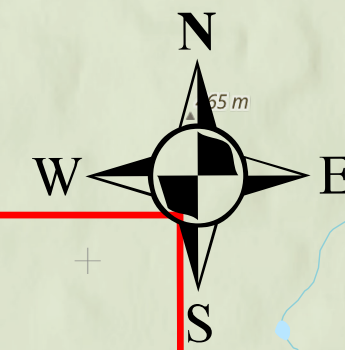
Scale: 1:35,000

0 0.350.7 1.4 2.1 2.8 3.5

Kilometers

Legend

- Mavis Lake Property
 - Flight Path Boundary
 - Mavis Lake Claim Cells
 - Mavis Lake Patent Claims
 - Township Boundary
- Utilities**
- Hydro Line
 - Natural Gas Pipeline
 - Submerged Hydro Line



APPENDIX C:
Claim Cells of Survey

Claim Cell	Issue Date	Anniversary Date	Due Date	Tenure Status	Claim Cell Type	HOLDER	Expenses Allocated (CAD)
341295	2018-04-10	2023-04-09	2023-04-09	Active	Single Cell Mining Claim	(100) Canada Critical Resources Corp.	\$25,000.00
101616	2018-04-10	2023-04-09	2023-04-09	Active	Single Cell Mining Claim	(100) Canada Critical Resources Corp.	\$25,000.00
101617	2018-04-10	2023-04-09	2023-04-09	Active	Single Cell Mining Claim	(100) Canada Critical Resources Corp.	\$25,000.00
101618	2018-04-10	2023-04-09	2023-04-09	Active	Single Cell Mining Claim	(100) Canada Critical Resources Corp.	\$25,000.00
101619	2018-04-10	2023-04-09	2023-04-09	Active	Single Cell Mining Claim	(100) Canada Critical Resources Corp.	\$23,804.00
160902	2018-04-10	2023-04-09	2023-04-09	Active	Single Cell Mining Claim	(100) Canada Critical Resources Corp.	\$800.00
166897	2018-04-10	2023-04-09	2023-04-09	Active	Single Cell Mining Claim	(100) Canada Critical Resources Corp.	\$800.00
179416	2018-04-10	2023-04-09	2023-04-09	Active	Single Cell Mining Claim	(100) Canada Critical Resources Corp.	\$800.00
179417	2018-04-10	2023-04-09	2023-04-09	Active	Single Cell Mining Claim	(100) Canada Critical Resources Corp.	\$800.00
179418	2018-04-10	2023-04-09	2023-04-09	Active	Single Cell Mining Claim	(100) Canada Critical Resources Corp.	\$800.00
179741	2018-04-10	2023-04-09	2023-04-09	Active	Single Cell Mining Claim	(100) Canada Critical Resources Corp.	\$800.00
186194	2018-04-10	2023-04-09	2023-04-09	Active	Single Cell Mining Claim	(100) Canada Critical Resources Corp.	\$800.00
196153	2018-04-10	2023-04-09	2023-04-09	Active	Single Cell Mining Claim	(100) Canada Critical Resources Corp.	\$800.00
196154	2018-04-10	2023-04-09	2023-04-09	Active	Single Cell Mining Claim	(100) Canada Critical Resources Corp.	\$800.00
205589	2018-04-10	2023-04-09	2023-04-09	Active	Single Cell Mining Claim	(100) Canada Critical Resources Corp.	\$800.00
215413	2018-04-10	2023-04-09	2023-04-09	Active	Single Cell Mining Claim	(100) Canada Critical Resources Corp.	\$800.00
233613	2018-04-10	2023-04-09	2023-04-09	Active	Single Cell Mining Claim	(100) Canada Critical Resources Corp.	\$800.00
233614	2018-04-10	2023-04-09	2023-04-09	Active	Single Cell Mining Claim	(100) Canada Critical Resources Corp.	\$800.00
234948	2018-04-10	2023-04-09	2023-04-09	Active	Single Cell Mining Claim	(100) Canada Critical Resources Corp.	\$800.00
253509	2018-04-10	2023-04-09	2023-04-09	Active	Single Cell Mining Claim	(100) Canada Critical Resources Corp.	\$800.00
253510	2018-04-10	2023-04-09	2023-04-09	Active	Single Cell Mining Claim	(100) Canada Critical Resources Corp.	\$800.00
270261	2018-04-10	2023-04-09	2023-04-09	Active	Single Cell Mining Claim	(100) Canada Critical Resources Corp.	\$800.00
271591	2018-04-10	2023-04-09	2023-04-09	Active	Single Cell Mining Claim	(100) Canada Critical Resources Corp.	\$800.00
290059	2018-04-10	2023-04-09	2023-04-09	Active	Single Cell Mining Claim	(100) Canada Critical Resources Corp.	\$800.00
290060	2018-04-10	2023-04-09	2023-04-09	Active	Single Cell Mining Claim	(100) Canada Critical Resources Corp.	\$800.00
302230	2018-04-10	2023-04-09	2023-04-09	Active	Single Cell Mining Claim	(100) Canada Critical Resources Corp.	\$800.00
330271	2018-04-10	2023-04-09	2023-04-09	Active	Single Cell Mining Claim	(100) Canada Critical Resources Corp.	\$800.00
340962	2018-04-10	2023-04-09	2023-04-09	Active	Single Cell Mining Claim	(100) Canada Critical Resources Corp.	\$800.00
341294	2018-04-10	2023-04-09	2023-04-09	Active	Single Cell Mining Claim	(100) Canada Critical Resources Corp.	\$800.00

APPENDIX D:

Expenses

Total \$143004.00

Expenses Table

Date	Supplier Name	Description	Total Amount CAD
2022-05-31	Southern Geoscience Consultants Pty Ltd	Interpretation - Litho-structural	\$ 46,955.00
2022-11-12	MPX Geophysics Ltd	Dryden Block (Ontario) Fixed Wing Survey Data Acquisition & Processing Payment of fifty percent (50%) of the Estimated Total to be payable on the Effective Date	\$ 96,049.00
		TOTAL	\$ 143,004.00